12-2004

MicroStrain Pattern Analysis of the Canine Patellar Tendon Following a Tibial Plateau Leveling Osteotomy

Joshua Paul Stapleton
University of Tennessee - Knoxville

To the Graduate Council:

I am submitting herewith a thesis written by Joshua Paul Stapleton entitled "MicroStrain Pattern Analysis of the Canine Patellar Tendon Following a Tibial Plateau Leveling Osteotomy." I have examined the final electronic copy of this thesis for form and content and recommend that it be accepted in partial fulfillment of the requirements for the degree of Master of Science, with a major in Engineering Science.

Jack Wasserman, Major Professor

We have read this thesis and recommend its acceptance:

Joseph Weigel, Richard Jendrucko

Accepted for the Council:
Carolyn R. Hodges

Vice Provost and Dean of the Graduate School

(Original signatures are on file with official student records.)

To the Graduate Council:

I am submitting herewith a thesis written by Joshua Paul Stapleton entitled "MicroStrain Pattern Analysis of the Canine Patellar Tendon Following a Tibial Plateau Leveling Osteotomy." I have examined the final electronic copy of this thesis for form and content and recommend that it be accepted in partial fulfillment of the requirements for the degree of Master of Science, with a major in Engineering Science.

Jack Wasserman

Major Professor

We have read this thesis and
recommend its acceptance:

Joseph Weigel

Richard Jendrucko

Accepted for the Council:

Anne Mayhew

Vice Chancellor and
Dean of Graduate Studies

(Original signatures are on file with official student records.)

MICROSTRAIN PATTERN ANALYSIS OF THE CANINE PATELLAR TENDON FOLLOWING A TIBIAL PLATEAU LEVELING OSTEOTOMY

A Thesis

Presented for the

Masters of Science

Degree

The University of Tennessee, Knoxville

Joshua Paul Stapleton

December 2004

Acknowledgements

I wish to thank all those who helped me complete my Master of Science degree in Engineering Science. I would like to thank Dr. Weigel, DVM, MS, University of Tennessee Veterinary Hospital, for all his assistance and guidance throughout my academic career. His effort to combine our fields for advanced improvement has made a lasting impression that I greatly appreciate. He has also provided me with needed experience to promote and advance my upcoming professional career. He was a caring and helpful mentor and I will be forever grateful for the opportunities he provided for me. I would also like to thank Dr. Jack Wasserman, PhD, University of Tennessee Department of Biomedical Engineering, for teaching the advanced biomechanics and helping with the soft tissue testing required for this project to be a success. Furthermore, I would like to thank Dr. Richard Jendrucko, PhD. His efforts to promote and advance the biomedical engineering program at the University of Tennessee have been invaluable with respect to helping mold the path of my professional career. I would also like to thank Dr. Monica Schmidt, PhD, DeRoyal, Inc., for be a true and caring mentor. She provided much needed guidance throughout not only my graduate, but undergraduate program as well. I would also like to thank all my colleagues at Smith & Nephew. They have given me a great opportunity to pursue my career in the manner that I desire. I would especially like to thank Stanley Tsai, MS, Smith & Nephew, Inc, Memphis, TN, whose help with the data acquisition was invaluable to the completion of this project.

Finally, I would like to thank my friends and loved ones, whose continued support made this work possible. While others said it was impossible, you continued your support and made the impossible, possible. Thank you.

Abstract

This study investigates the change in strain patterns of the canine patellar tendon following a Tibial Plateau Leveling Osteotomy (TPLO). The TPLO is a procedure used to minimize anterior tibial translation in canines following a cranial cruciate rupture. A noted clinical deficiency randomly seen with the TPLO is an inflammation of the patellar tendon. In some instances, the inflammation results in material damage resulting in a calcification of the tendon and in worst cases, a fracture of the patella.

In order to investigate the strain patterns, four fresh frozen canine cadaver stifles were used. The cadavers were mounted for stabilization and a motor was attached to the patella to simulate the quadriceps contraction. Tendonous material is not ideal for direct measurement of strain; therefore, a rectangular rubber section was attached to the anterior patella and the insertion of the quadriceps femoris complex of the anterior tibial crest. A strain gage was then applied to the center of the rubber aligned axially with the line of applied force. The stifle was put through a simulated extension using the motor attached to the patella. A controlled intact knee was used as the baseline for all four specimens, independently. Following the control data acquisition, a simulated cranial cruciate rupture was performed and the strain values collected in the same manner. Finally, the TPLO was performed. Two specimens used an 18 mm biradial saw, whereas, the other two used a 24 mm biradial saw. Five measurements of strain were recorded for the control, a simulated ruptured cranial cruciate, and 0, 2, 4, 6, 8, 10, 12, and 14 mm of tibial plateau rotation following a TPLO.

It was found that there is a statistically significant increase in strain experienced by the patellar tendon following a TPLO at nearly every angle of rotation for both cuts. Whereas, a simulated ruptured cranial cruciate ligament

resulted in no statistically significant difference in 3 out of 4 of the samples. Strain values increased by as much as 96 and 81 percent for the 18 mm cut at 8 mm of rotation and the 24 mm cut at 12 mm of rotation, respectively.

This study will provide a basis for improvements to be made with respect to the TPLO. Further research may result in a more concise and clinically relevant data set that will continue the advancement of this common surgical technique.

Preface

This study examines the Tibial Plateau Leveling Osteotomy for cranial cruciate repair in canines. The procedure examined is highly used in veterinary medicine and continued scientific investigation is needed to reform and perfect the procedure. This study also represents the combined work of the University of Tennessee Veterinary Hospital and the Biomedical Engineering program. A continued development of this relationship will certainly lead to an improvement for both institutions.

Table of Contents

List of Tables

List of Figures

Nomenclature

CCL	Cranial Cruciate Ligament
TPLO	Tibial Plateau Leveling Osteotomy
DAQ	Data Acquisition
PC	Personal Computer
DC	Direct Current
HP	Horse Power
SD	Standard Deviation
PT	Patellar Tendon
Mea.	Measurement
Rot.	Rotation
mm	Millimeter
kgs	Kilograms
lbf	Pound-force
lbs	Pounds
in	Inches
mm/min	Millimeters per Minute
in/min	Inches per Minute
RPM	Revolutions per Minute
V_{ex}	Excitation Voltage

Chapter 1: The Canine Stifle: A Ligament Overview

The function of the stifle is a complex reaction of the existing anatomical components. The patella, femur, tibia, ligaments, tendons and menisci all perform an essential function within the joint capsule and a failure of any one can result in deterioration and ultimately, a reduction of joint use. The ligaments are particular vulnerable due to the repetitive loading patterns and their complex loading geometry. Unlike the human knee, the canine stifle, although anatomically similar, must support a much higher level of stress. The geometry of the stifle provides this added force. Whereas the human knee is aligned with the axes of weight bearing with only minimal valgus or varus misalignment, the canine stifle is loaded axially while being in more of a pre-flexion position. Therefore, the load on the canine stifle is considerably higher per unit weight than that seen by the human knee.

Ligaments are composed of water and collagen fibers that run in the longitudinal axis parallel with the axis of loading. The collagen is primarily Type I and Type III, with traces of Types V, X, XII, and XIV. Other proteins are present, but in minute, negligible amounts. The ligament fibers are surrounded by water and proteoglycans, which aid in the lubrication providing a means of slide-ability for the fibers. It is this sliding that allows for the ligament to endure strain values as high as ten (10) percent. The fibers act as a crimping mechanism and lengthen in groups as the ligament is strained to provide increasing support. During normal activity, the ligaments are easily elongated to maintain normal kinematics, but with higher applied external loading, the ligament stiffness increases to provide added support in restricting the macro-motion of the joint [30]. However, in canines, the maximum load is approached more often than not, increasing the risk of

ligament damage. In general, canines are extremely active and provide an increased loading pattern on the ligaments of the knee on a regular basis.

The canine stifle is comprised of seven major ligaments: the cranial and caudal cruciates, lateral and medial collateral, the meniscofemoral, the patellar tendon/ligament and the caudal fibular ligaments as shown in Figure B-1[1]. Only the cranial cruciate ligament (CCL) and the patellar tendon, as they will be referred to for the remainder of this paper, will be examined in depth for this study. The four primary stabilizing ligaments are the medial and lateral collaterals, and the caudal and cranial cruciates. The medial and lateral collaterals are located on the surrounding exterior of the stifle joint capsule. The caudal and cranial cruciate ligaments are found within the femorotibial joint. Fibers composing the cranial cruciate ligament originate on the medial face of the lateral aspect of the femoral condyle. The CCL transverses cranially, medially, and distally to insert onto the cranial intercondylar region of the tibia. The CCL is composed of two bands, the craniomedial and caudolateral. The CCL receives its' blood supply from the surrounding synovial tissue [37].

Virtually every stifle or knee injury involves a low-degree sprain of one or more of the ligaments within the knee [36]. Because the ligaments fail to heal properly, repetitive micro-trauma can result in a fatigue failure. An injury of the CCL can lead to knee instability associated with damage to other knee structures and the increased risk of degenerative joint disease [36]. Furthermore, the resulting pain from the stressed ligaments may cause an alteration in gait. This kinematic change may be detrimental to the structure and function of both the injured and contra lateral knees. Research has shown that approximately one-third of patients with a cranial cruciate rupture

[1] All Figures are located in Appendix B

develop ligament damage in the contra-lateral leg within a year-and-a-half after surgical reconstruction or a geometrical alteration [38].

The cruciate ligaments in the knee joint, in combination, define and sustain the motion of the tibia relative to the femur [12]. In addition the CCL is the primary restraint acting to prevent anterior subluxation of the tibia on the femur [35]. Due to the geometry and kinematics of the canine stifle, the CCL is critical to total knee stability. CCL rupture is a partial or complete tear of the CCL resulting in joint instability, pain, and lameness. When ruptured, the anterior tibial subluxation is magnified by the geometry of the stifle, causing vast amounts of structural damage from the resulting macro motion of the knee. Instead of healing, the torn ligaments will retract towards the proximal femur. This usually results in degenerative joint disease in the stifle, ultimately leading to a reduction, or in some cases, total functional loss of the joint. It is important to note that the stifle does not only move in the proximal-distal direction of the applied load, but motion can also occur in all the anterior-posterior, varus-valgus, internal-external rotational, and medial lateral directions [30]. Therefore, non-restricted motion in one plane can lead to an increased loading pattern for the ligaments that are restricting motion in other planes. This increased loading in multiple degrees of freedom has been shown to result in a physiological remodeling of the tibial plateau. The research of Morris and Lipowitz showed that canines with CCL ruptures have a significantly greater tibial plateau angle than those without injury [42].

Chapter 2: Tibial Plateau Leveling Osteotomy (TPLO) for Cranial Cruciate Rupture Repair in Canines

Following a rupture of the CCL, it must be repaired, replaced, or effectively neutralized in order to reduce the resulting macro motion caused by instability of the stifle. Due to the geometry of the canine stifle, the anterior tibial translation with respect to the femur is magnified leading to impingement of the caudal horn of the medial meniscus [41]. In effect, the femur will slip off the posterior aspect of the tibia. This motion is detrimental to the joint and may ultimately lead to a non-functional joint without treatment.

There are several treatments available for the repair of a CCL rupture, including, but not limited to, a suture replacement, graft replacement, and a Tibial Plateau Leveling Osteotomy (TPLO). The TPLO will be examined for this study; therefore it will be focused on primarily. The TPLO, Tibial Plateau Leveling Osteotomy, was designed and patented by Dr. Barclay Slocum, DVM. It is a surgical technique, US Patent No. 4,677,973, with licenses available from Slocum Enterprises in Eugene, OR. The objective of the procedure is to reduce the anterior cranial tibial thrust resulting from a cranial cruciate ligament rupture in the canine stifle. As weight bearing forces are transmitted across the femorotibial joint, they can be resolved into compressive and cranial components. Cranial tibial thrust provides an explanation to the unsatisfactory results of autograft and suture replacements. When the cranial cruciate ligament is replaced, the stifle must undergo a healing process. During that time, the forces through the stifle are solely placed upon the replacement material [41]. The implanted material experiences such high, repetitive loading which commonly leads to failure. Furthermore, these replacements carry a higher risk of infection, abrasion can

lead to ‘sterile effusions’, and the ligament material tends to creep with time [17]. The TPLO attempts to reduce the cranial tibial thrust by changing the geometry of the stifle. Taking an osteotomy of the proximal tibia can reduce the cranial tibial thrust. Following the osteotomy, the tibial plateau can be rotated to change the geometry of the tibia to be more level with regards to the femur. This enhances the effectiveness of the active forces of the stifle flexors of the thigh by aligning the anatomical forces into a more neutral axis [39]. This procedure allows the joint to heal by reducing the effective cranial tibial thrust resulting in lower overall joint loading.

As previously stated, the stifle joint can be divided into two orthogonal components: a compressive force parallel to the loading axis of the tibia and a cranially oriented shear force called the cranial tibial thrust. The magnitude of the cranial tibial thrust is a function of both the slope of the tibial plateau and the magnitude of the compressive force along the loading axis of the tibia [40]. Ideally, the magnitude of this loading would be minimized by aligning the axis of applied load to eliminate one of the planar components resulting in a singular compressive load. The resulting anatomical alignment allows tibial compression to become the primary forces seen within the joint, thus minimizing the resulting force applied to the ligaments during weight bearing. The resisting force to the tibial thrust involved is the cranial cruciate ligament. When ruptured, the kinematics of the knee are changed, resulting in the caudal cruciate ligament being solely responsible for stabilizing the knee [43]. Therefore, the resulting compressive force seen by the stifle is magnified by the relative translation of this applied force into a more load-bearing axis. Because of these joint reactions, a TPLO is administered to return the joint to a more physiological function.

An incision is extended over the craniomedial surface of the limb, from the proximal aspect of the patella to the proximal third of the tibia. Either a

full medial parapatellar arthrotomy or a limited caudomedial arthrotomy can now be done to allow greater relative motion of the meniscus. The medial aspect of the proximal tibia is exposed by incision of the caudal belly of the sartorius muscle and relevant moving of the surrounding gracilis and semitendenosus muscle complexes. The popliteal muscle, artery, and vein are carefully elevated to prevent iatrogenic damage. A patented armamentarium, including a tibial jig and biradial saw, is used to create a proximal tibial crescent-shaped osteotomy. The saws have different diameters to accommodate different sizes of tibial metaphyses. Before the osteotomy, the bone is marked on the distal aspect of the tibia, directly along where the osteotomy is to be performed, in 2 mm increments. A single mark is placed at the osteotomy site on the plateau to be transected. Using the biradial saw, the tibial plateau is cut to allow a pivoting crest created for rotational leveling. This cut has the distinct biomechanical advantage of maintaining the position of the tibial plateau in the sagittal plane while limiting the risk of tibial crest fracture and poor plate positioning. The magnitude of the tibial plateau rotation is based on the preoperative radiographic measurement of the tibial plateau slope angle. This slope can be converted into a chord length, depending on the radius of the saw blade, by the formula, $C = 2R(\sin[\alpha/2])$ where C is the length of the chord intercepted by an angle α, equal to the measured tibial plateau slope angle, and R is the radius of the saw blade. Once an optimal geometrical angle is determined, the wedge is rotated to match the resulting reference mark on the distal aspect of the osteotomy, thus resulting in a leveling of the tibial plateau. The appropriate plate and bone screws are used to stabilize the osteotomy for healing while maintaining the new orientation [39, 40].

Chapter 3: Patellar Tendon Structure and Function

The patellar tendon is one of the more intriguing materials in physiology. One of the more debated "medical terms" involves the patellar tendon and directly involves its' unique nature. Throughout medical literature, the patellar tendon is also commonly referred to as the patellar ligament. A tendon is defined as: connective tissue bonding muscle to bone. A ligament is defined as: connective tissue bonding bone to bone [30]. The patellar tendon is the connective tissue for the quadriceps femoris complex and encapsulates the patella, which provides a means for patellar traction [31]. It is the proximal attachment for the extensors of the knee to the tibia. So it has become a personal preference as to what physicians and surgeons refer to the tissue as. For the purposes of conformity, this study will refer to it as the patellar tendon.

The application of the patellar tendon for medical device use is of great importance. Current research involving joint replacements attempts to mimic how the body originally functioned. In order to accomplish this, the material and structural properties of the original material, must be evaluated [34]. As stated before, the patellar tendon is the attachment for the quadriceps femoris to the tibial crest and provides a means for patellar traction. A radiograph of a healthy, intact knee is presented in Figure B-2. In the case of a ruptured or transected patellar tendon, the patella will move axially towards the proximal femur as shown in Figure B-3. This can cause several injuries due to the loss of patellar traction and the instability of the knee. More importantly, the knee will fail to function properly because of the loss of extension.

The patellar tendon represents the pinnacle for material performance. Science has yet to develop a material that can withstand repetitive loadings at such a high volume for such a substantial amount of time. Where

manufactured materials typically prosper from underutilization, it has been shown that the patellar tendon fails under less utilization [8]. But more importantly, the tendon has the ability to translate its loading patterns through different axial channels if an area is over-fatigued or even structurally compromised [8].

Biologic materials present a multitude of difficulties when trying to find a comparable manufactured material to restore physiological function. There are no standardized values for the mechanical properties of a tendon. The properties change with regards to health, age, structure, integrity, intrinsic kinematics resulting from surrounding connective tissues, and overall conditioning, in some ways like that of a manufactured material, but do not conform to a well defined and standardized model. The health of a subject is always a highly contributing factor to the properties of the patellar tendon and presents a problem for this standardization of the material properties. Along with the health, the overall condition of the tissue is an important factor. Patients who are highly active tend to have more energy transfer into their muscles directly resulting in a thicker, denser patellar tendon [18]. Furthermore, the kinematics of a canine stifle cause increased strain rates and maximum levels, which are responsible for increased trauma. Aging of the tissue is yet another major consideration that has not been fully investigated. Material integrity is a major contributing factor to the mechanical properties of the patellar tendon. When an area of the tendon is compromised, loading patterns will change allowing a reduced stress zone around the injured section providing an opportunity for healing to occur [28]. While this results in a relaxation of the tendon in the damaged areas, it also results in an increased loading on the uncompromised sections, which may result in failure there as well.

Intrinsic kinematics is yet another contributing factor to the difficulty of modeling the mechanical properties of the patellar tendon. Kinematics, physiologically, describes the motion of diarthroidal joints as well as locomotion and gait. Unlike the hip, the knee does not offer a great deal of intrinsic boney stability. The knee relies on the encapsulating ligaments and tendons along with the alignment of the weight bearing force to supply stability to the joint [27]. One of the more important factors to recognize is that the knee does not move only in the direction of the applied load, but medial-lateral motion and internal-external rotation can also occur [23].

One of the most prominent uses for the patellar tendon in modern medicine is the one-third bone-patellar tendon-bone autograft for cranial cruciate and more so, anterior cruciate ligament reconstructions [15]. Studies have shown that while the tendon is very strong, it weakens considerably when grafted as a substitute for the cranial cruciate ligament due to the distinct material property differences [11, 13]. The biologic and biomechanical properties have also been shown to change with the absence of the surrounding nutritional environment and the presence of tissue necrosis commonly associated with *in situ* freezing for later experimentation [16]. Yet another problem associated with the one-third bone-patellar tendon-bone autograft is the decrease in patellofemoral contact area resulting from the procedure. Chan et al. discovered that following the patellar tendon transection, the patellofemoral contact area decreased from the resulting instability of the knee [31]. The decrease in contact area will directly result in an increase in stress on the patella. Because of the inadequate biomechanical properties following a transection and other problems resulting from a graft procedure, alternative methods where developed in an attempt to improve joint stability without removing the soft tissues within the joint. The research to achieve this joint stability resulted in the creation of the TPLO.

Structurally, tendons are bright white, parallel rope-like structures containing collagen fibrils, fibril bundles, fascicles and tendon units that run parallel to the geometrical axis of loading [30]. The patellar tendon is composed primarily of fiber forming type I collagen and functions to store and transmit elastic strain energy during extension of the stifle resulting from quadriceps femoris complex contraction [12]. Proteoglycans and hyaluronan are additional macromolecules present that occupy the aqueous spaces between fibrils limiting tissue collapse. In mature tendon, proteoglycan filaments are orthogonally arranged in the matrix surrounding collagen fibrils suggesting that these elements are involved in force transmission [5]. Tendons have been shown to undergo remodeling during increasing stress. It is the hypothesized that the properties of tendons can be modeled according to such structural properties as a combination of their cross sectional area, structural remodeling, biochemical, and the muscle-tendon complex reactions [4, 31, 32].

The primary mechanical property of the patellar tendon to be investigated in this study is the maximum strain. The reason for isolating the maximum strain is that tendon and ligament failure stresses change during development and adaptation, but failure strains have been shown to remain the same [14]. Strain is also a material constant that will only change as the modulus and cross sectional area of the tendon change. To remedy the differences between samples, a rubber replacement will be used over top of the tendon as explained later. The strain will be determined by mechanical loading in terms of the strain created during physical activity throughout the range of motion and primarily at the end range of motion for extension where the patellar tendon strain will be the highest [9].

The patellar tendon has been shown to withstand a high amount of strain, sometimes reaching as high as twenty percent elongation [20]. This

characteristic is that which separates the patellar tendon from other materials; it can be stiff, yet elastic too. The repetitive micro trauma is overcome by translating the strain across the separate collagen fibrils. When a fibril loses structural integrity, the remaining fibrils assume more load to allow remodeling and repair [15]. However, quadriceps muscle weakness has been shown after patellar tendon damage suggesting that the muscle assumes some of the offset loading as well [10].

During movement, muscle work is lost through not only the resulting motion, but friction, plastic deformation of tissue, and involuntary contractions resulting in opposite muscle forces as well. At the same time, some of the mechanical energy generated or resisted by the muscles is conserved due to work against the conservative forces of the elastic structures in the body [6]. The tendon structures play a very important role in the transmission of tension from muscle fiber to bone. A clinically relevant problem involving the TPLO is an occurrence of inflammation within the patellar tendon in some patients. This inflammation can become so bad that the trauma to the patellar tendon cannot be repaired by the body fast enough with respect to the resulting damage, which leads to a callus forming around the tendon. In some extreme cases, the patellar tendon can actually calcify. Because of the role the tendon plays involving transmission of the muscle forces to the attached bones, this calcification can result in a complete fracture of the patella as presented in Figure B-4 (B-4). In order for the patellar tendon to function properly, it must provide a means of dampening the force translated through it from the quadriceps during extension. It is for the preceding reasons that the patellar tendon has been classified as a viscoelastic material [7]. The viscoelastic properties have been studied extensively using isolated animal or human tendonous material undergoing elongation to failure. However, it is likely that tendon structures *in vivo* differ substantially from

those of cadavers in both dimensional and mechanical properties due to differences in size, age and storing procedures [26].

In vivo testing is a major obstacle to obtaining quality and reproducible tendon data. While ideally, *in vivo* testing will lead to the best possible physiological results, it is more often than not unpractical for most applications. When dealing with a live environment, too many variables result in an uncontrollable experiment that is unable to result in a statistical significant conclusion. Such variables as muscular fatigue, thermal variance, data acquisition failure due to environmental issues, altered kinematics resulting from residual pain, patient availability, and residual tissue damage become too overwhelming to control. These problems tend to lead most of the mechanical testing for mechanical properties of the patellar tendon and other biological tissues, to be performed in a laboratory setting *in vitro*.

The strain in the patellar tendon is commonly found in two manners. The first method is to transect the tendon and perform mechanical tension testing using an axial load-testing frame such as an Instron (Instron Co., MA) or an MTS (MTS Systems Corp, Eden Prairie, MN). The loading frames will apply a displacement control test, which loads the tendon to failure while plotting the resulting load versus displacement curve and recording the time. While accurate and practical, the combination of transection and freezing of the patellar tendon can present anomalies and has adverse affects on the mechanical properties [17, 19, 28]. Furthermore, this is not representative of the physiological loading the tendon undergoes. During extension of the leg, the patellar tendons primary functions are to provide an attachment for the extensors of the knee to the tibia and to provide a means of patellar traction. Therefore, while the tendon does see a tensile component, it is not solely an axial function. The complex geometry of the knee allows for multidimensional motion and loading which, if unaccounted for, gives a

misrepresentation of the loading pattern seen during weight bearing by the tendon. While the test will provide a modulus of elasticity for tendonous material, it will not characterize a true loading pattern as seen during physiological action.

Another alternative for measurement of the strain the patellar tendon undergoes is by using strain gauges for data acquisition. While you may or may not use a strain gauge *in vivo*, you can use it *in vitro* without having to transect the tendon. A strain gage will give a measurement of resistance change for the resulting deformation the tendon undergoes during a weight bearing simulation. Using this data along with known geometrical properties of the tendon, a more unique loading pattern accustomed to the kinematics of the tendon can be created. New technology has also increased the base of knowledge for strain measurement. Imaging technology allows for small micro-measurements to be taken with high speed, high resolution cameras that will provide not only a two-dimensional analysis of the loading patterns, but the resulting orthogonal deformation of the tendon, allowing a three-dimensional strain field to be created. Liquid metal strain gages are also a new developing technology. They consist of a solid polymer tube containing mercury. As the tube is displaced, the cross sectional area of the mercury is changed resulting in a change in resistance which can be converted to a measurement of strain.

A low strain non-linear "toe region", a linear region, and a nonlinear yield and failure region as presented in Figure B-5 are characteristic of the stress-strain curve of the patellar tendon. The low strain toe region has been shown to involve a dampening effect provided by the collagen fibrils and fibers, initiation of stretching of the collagen triple helix, and molecular slippage [12]. In the linear region molecular stretching and molecular and fibrillar slippage are the predominate modes of deformation which lead to failure in

the yield and failure region after crosslinks between the fibrils break. Therefore, to refrain from plastic micro trauma, normal strain levels for the patellar tendon should stay between one to five percent elongations as shown in Figure B-5. Yet in some cases, end range-of-motion flexion during strenuous activities can reach up to or near one hundred and seventy degrees, which likely extends the patellar tendon beyond these ideal elongations [9, 21, 25].

Chapter 4: Strain Gage Theory and Application

The metallic strain gage consists of a very fine wire or, more commonly, metallic foil arranged in a grid pattern [1]. Theoretically, a single wire could be used to measure the change in resistance as the wire is displaced. The grid pattern in strain gages maximizes the amount of metallic wire or foil subject to displacement in the parallel direction, in effect, amplifying the signal as shown in Figure B-6. The cross sectional area of the grid is minimized to reduce any effects of shear and Poisson Strain. The grid is bonded to a thin backing, called the carrier, which can be attached by cyanoacrylate directly to the specimen to be measured. Due to the carrier being bonded, and not the grid, the strain experienced by the medium is transferred directly to the strain gage, resulting in a change in a deformation of the grid wires. This deformation results in a change in electrical resistance across the gage. As mentioned before, an alternative to the metal foil gage is the liquid mercury strain gauge. The liquid gage has a defined cross sectional tubular area. The leads are attached at the origin and insertion of the patellar tendon and the change in electrical resistance is related to the change in cross sectional area to give the resulting strain [29]. Strain gages are available commercially with nominal resistance values from 30 to 3000 Ω, with 120, 350, and 1000 Ω being the most common values.

In practice, the strain measurements rarely involve quantities larger than a few microstrains ($ex10^{-6}$). Therefore, in some instances, to measure the strain requires accurate measurement of very small changes in resistance [1]. This is especially seen at the insertion on the tibial plateau of the patellar tendon as the material properties directly related to the collagen content vary as one moves proximally along the tendon, resulting in values that can be much

larger at the musculotendon complex. To measure such small changes in resistance, strain gauges are used in a bridge configuration with a voltage excitation source. The Wheatstone bridge, developed by Sir Charles Wheatstone, 1843, consists of four resistive arms with an excitation voltage, V_{ex}, that is applied across the bridge as shown in Figure B-7 [1]. The output voltage of the bridge, V_o, is $V_o = [(R_3/(R_3 + R_4)) - (R_2/(R_1 + R_2))] * V_{ex}$. From this equation, it is apparent that when $R_1/R_2 = R_4/R_3$, the voltage output V_o will be zero. Under these conditions, the bridge is said to be "balanced" [2]. So a change in resistance in any arm of the bridge will result in a non-zero output voltage, which can be manipulated into an engineering equation [2].

A full bridge consists of four gages capable of seeing a resistance change. For many applications, a full bridge is not applicable. It may be due to space limitations or difficulty of application. In these situations a half or quarter bridge may be used. The same theory applies using a Wheatstone half or quarter bridge, but in place of the missing gages are resistors with constant and equal nominal resistances. Since these resistors will not change the resistance output, any change by the active gage(s) will result in an unbalanced bridge voltage, which can be manipulated into a measured strain. The quarter bridge is not desirable for most applications, other than a direct axial loading pattern. If the gauge is placed on a curved surface, the gage will read out of phase due to the geometry. This problem can be corrected by adding a second gage perpendicular to the primary gage, which returns a measurement for the Poisson strain. If a quarter bridge is the only means of measurement, problems can occur with the sensitivity. The resistors will remain constant, but this pre-strained position of the gage results in a non-zeroed point of interest. This can be balanced using a potentiometer, but as an offset voltage is applied to the system, not only does the sensitivity of the system decrease, but the noise increases, and the gage may near the maximum

readable resistance change as well. Therefore, it is common to use a half bridge orientation with a dummy gauge for most applications. By placing the dummy gage on a similar geometrically oriented surface, the bridge is rebalanced with the two known resistors on opposite ends and the two open gages under similar, if not the same, strain resulting in a balanced bridge. When applying the dummy gage, it may become difficult to obtain the exact geometric position as that of the test gage. Again, a potentiometer may be placed into the bridge allowing a balancing voltage to be added or withdrawn providing the bridge balance.

In some instances, the principle stress axes are unknown or too geometrically undefined to locate with any confidence for statistical repeatability. In order to locate these principle axes, a strain gage rosette is used similar to the rosette shown in Figure B-8. A rosette takes three simultaneous strain measurements at known angles, usually forty-five or sixty degrees. Using the three resulting strain values, the principle axes can be identified and located by proportional mathematics. This reduces the error associated with attachment of the gage being incorrectly aligned with the applied load, allowing for more accurate and statistically significant data to be recorded [3].

Once the gage setup is determined, each gage is attached to a signal-conditioning box to amplify the small resistance change and wired to a data acquisition card (DAQ) on the back of a PC. The data is read by specialized software packages and calculations can be performed on the primary interests [3].

Chapter 5: Experimental Hypothesis

The patellar tendon will experience a change in strain as the tibial plateau geometry is altered following a Tibial Plateau Leveling Osteotomy. It is this change in strain that will be evaluated for the TPLO. By simulation of weight bearing before and after the simulated cranial cruciate rupture and the resulting surgical procedure, strain analysis will provide a pattern of increased or decreased loading as seen by the patellar tendon with respect to the amount of applied rotation to the tibial plateau. This data will provide a basis for understanding the pathology of patellar tendon inflammation, as seen in some patients, after a TPLO.

This research will provide a better understanding of the TPLO procedure and the resulting effects on the patellar tendon. It will also serve as a basis for future work, in order to further investigate this common procedure.

Chapter 6: Materials Used and Methods

Materials:

- Specimen 1: Canine, Left Leg, 39.3 lbs (17.8 kg), ~1 year old – 18 mm cut
- Specimen 2: Canine, Right Leg, 63 lbs (28.6 kg), ~2 years old – 18 mm cut
- Specimen 3: Canine, Right Leg, 66.8 lbs (30.3 kg), ~2-3 years old – 24 mm cut
- Specimen 4: Canine, Left Leg, 63 lbs (28.6 kg), ~2 years old – 24 mm cut
- SC-2043-SG Data Acquisition Board – National Instruments Inc., Austin, TX
    - Model # 2043-SG
- Data Acquisition Card – National Instruments Inc., Austin, TX
    - Model # MIO-16XE
- Personal Computer, Gateway Inc, Poway, CA
    - Model # 2000 E4200 PII
- Insulated Copper Wire
- Soldering Iron – 25W Weller
- Strain Gages – MicroMeasurments, Inc., Raleigh, NC
    - Model # CEA-13-062UW-350
- LabVIEW® – National Instruments, Austin, TX
    - Version 6.1
    - MAX 2.2 – Measurement and Automation Explorer
- M-Bond 200 adhesive kit – MicroMeasurements, Inc., Raleigh, NC
- Microsoft Office Software Package – Microsoft Inc., Redmond, WA

- 0.105“ x 0.7535“ x Physiologically determined” solid rubber vacuum belts – Hoover Inc., N Canton, OH
    - Model # 38528-835
- Servo Motor - 25 RPM
- Two 6 Volt DC Power Sources – Rayovak Inc., Atlanta, GA
- Other: 2x4 Wood, Standard Metal C-clamps, High tension metal wire, Digital level
- All standard surgical equipment to perform a TPLO

Methods:

The study plan for testing is presented in Appendix C.

Four specimens of canine cadaver stifles were transected and frozen prior to evaluation. Upon testing date, the cadaver stifles were thawed to room temperature and tested immediately to reduce the affective necrosis. The cadavers were screw mounted to a C-clamped wood block, used for stabilization, onto an operating table as presented in Figure B-9. The cadavers were oriented to ninety degrees of flexion at the stifle to begin testing. The distal aspect of the leg, below the knee, was off the edge of the operating table to provide a constant resistive force relative to the weight of each specimen. The surrounding tissue was pulled away or removed to allow a clear line of sight and clean working area around the patellar tendon. Careful attention was made not to surgically disrupt the integrity of the tendon. The objective of this testing was to isolate the patellar tendon and record the resulting strain patterns under a simulated cranial cruciate rupture, and zero, two, four, six, eight, ten, twelve, and fourteen millimeters of rotation following a TPLO. In order to accomplish this, a physiological simulation of loading had to be determined. The mechanical mechanism of extension of the knee is provided by the quadriceps femoris. The quadriceps femoris inserts onto the proximal

patella and the patellar tendon connects the distal patella to the tibial crest. To create this simulation, a bone screw was attached directly to the anterior patella to provide an attachment for high tension steel wire to pull the patella using the servomotor simulating the quadriceps femoris musculotendonous complex as presented in Figure B-10. Some patellar traction problems arose with samples 3 and 4, resulting in two new attachments to the patella. A bone screw was placed on both the medial and lateral aspects of the patella to provide an attachment for high-tension steel wires to pull the patella in a more controlled simulation of the quadriceps femoris musculotendonous complex. Having the sides stabilized and the force applied to the anterior patella, the tracking was mechanically provided reducing the internal rotation. In both cases, a castor wheel, which was grinded down through the center aspect of the circumference of the wheel to provide a tracking for the wire, was screwed directly onto the mid-aspect of the femoral shaft as presented in Figure B-11. The castor acted as a pulley system guiding the wire to a servomotor powered by twelve volts DC. The servo motor was altered to have a steel winding wheel attached to the output shaft of the motor, as shown in Figure B-12, to provide more structural support to the system and reduce slippage by increasing the surface area of contact between the wire and wheel. The motor ran at a speed of 25 RPM for the duration of testing.

The original study plan was written to apply the strain gages directly to the mid-aspect of patellar tendon between the insertion and attachment at the distal patella. The gage carrier had a good attachment to the tendon, as presented in Figure B-13, but a tendon is not a uniformly homogenous material. The surrounding synovial sheath, which provides material protection for the tendon, is more stiff and misrepresentative of the strain patterns the tendon undergoes as a whole. To remedy this situation, a uniform (0.105” x 0.7535” x Physiologically determined) rectangular section of rubber

was attached to the anterior mid-aspect of the patella and directly to the tibial crest at the insertion of the patellar tendon using two eye screws drilled into the cortical bone as shown in Figure B-14. When using a strain gage, the voltage difference is essentially meaningless. It is a function of multiple factor input by the recorder. To allow for a meaning to be applied to the value of strain returned for measurement, some sort of calibration and validation procedure must be performed. To validate the gages and the carrying medium, rubber, a displacement control tension test was completed using an 858 MiniBionics MTS with a 200 lbs load cell. The testing setup, as presented in Appendix D[2], used to wedge grips that tighten under tension. One strain gage was aligned parallel with the long edges of the rubber to provide the closest possible measurement to the principle axis. A load control test was then performed at 0.1 in/min (2.54 mm/min) until the gage reached the maximum readable strain. This value was then plotted against the outputted load, recorded from the MTS using TestStar, to obtain a load versus deformation curve. By extrapolating from this curve, a modulus for the rubber could be determined and the actual strain values calibrated with respect to the amount of displacement undergone by the section.

For this study, the primary objective became the changing strain pattern as it relates to an intact knee, not the actual value seen by the tendon. Prior research has been focused on defining a value for the strain seen by the patellar tendon. After examining the problem statement, it was determined that the value is irrelevant to this study. The primary concern is the change the patellar tendon undergoes following a TPLO. Therefore, the rubber was a suitable alternative to determine any changes in this pattern resulting from the instability of the knee after a CCL transection and the TPLO procedure. The

[2] The test set up and recorded data are shown in Appendix D. This became an area of testing that, while possibly important for future work, was not relevant to this study.

rubber was chosen to be a taught material to ensure the rubber was carrying the load rather than the tendon.

Once the rubber attachment was made, a single strain gage was attached using the M-bond 200 epoxy from MicroMeasurments, Inc. The gage was captured using ordinary cellophane tape. The M-bond and catalyst were applied to the area of interest on the rubber and then the gage was uniformly pressed onto the area with the tape so the wires were not affected by the epoxy. After allowing approximately a minute for the adhesive to take, the tape was removed leaving the gage intact on the specimen. The gage was aligned in an axial direction along with the physiological loading characteristic for the patellar tendon. Care was taken to ensure that the axis was aligned properly using a digital level.

The strain gages were set up in a half bridge orientation. The primary gage was attached directly to the rubber simulating the patellar tendon. In order to receive a readable resistance change, a 'dummy' gage was attached to a similar piece of rubber and laid to the side, as to avert any motion. The DAQ board had two built-in 350 Ω resistors that served as the completion for the other half of the bridge. As the rubber changed orientation during motion, the gage length underwent a resulting deformation offsetting the balance of the bridge. The gage designation and engineering data sheet is shown in Figure B-15. Shielded copper wires, approximately five feet in length, were soldered to the attached copper gage terminals. The shielding prevented noise from entering the signal due to the length of the wires. An excitation voltage of 3.33 V was applied to the active gage and an excitation voltage of -3.33 V was applied to the dummy gage. The gages were connected to the positive output channel on the DAQ board, which read the resistance change across the bridge. The electrical designation was set to be a non-referenced single ended

signal. The analog voltage was then converted to a digital output using the DAQ card in the back of the PC controlled by LabVIEW®.

LabVIEW® is a programming language designed for technical application program writing. The LabVIEW® programs for data acquisition are shown in Figures B-16 and B-17. An input signal, usually a voltage change, is recorded and wired into the DAQ card. The program defines this input signal and a filter is set to gather all signals from any predesignated active channels. The program for this study used only one channel because only one reading was taken for each measurement. From the analog input voltage, an index array is created that, while coupled with a time counter, creates an indexed matrix array of values as pertaining to the inputted cycle count. The programs data acquisition frequency was set at 20 Hz due to the short period of testing. From the resulting index array, a functional waveform component is defined and then put back into a new array as an X-Y Cartesian system. Using the defined voltage values coupled with their timing indicators, the program performs any designated calculations to transform the input voltage into a strain measurement versus time. By inputting the bridge voltage, gage factor, and any voltage zero offsets, the program converts the analog voltage signal into a digital strain reading. After converting the voltage change to a strain measurement, the values are built into a final array and sent to a text and waveform compiler. With the scan rate and strain measurements, the program concatenates the strings with predefined controllers to create a readable output file, which was then sent to Microsoft Excel for examination. The controllers are just a computer designation denoted as 0, 1, 2, 3, etc. to allow the computer to identify separate signals.

Using the servomotor powered by a 12-volt DC power source running at a speed of 25 RPM, the attached wire tensioned, resulting in a simulated full extensional force applied by the quadriceps femoris across the stifle. A strain

measurement was recorded throughout the range of motion and referenced to the cycle time. The surgical setup for the TPLO is presented in Figure B-18. The metallic jig was used for stabilizing the two bones after the osteotomy while the screws in the anterior and lateral directions are used to hold the cut tibial sections in place, instead of attaching a plate with screws each time. For each specimen, a group of N=5 measurements were taken for an intact knee, a cut cranial cruciate, and each of the corresponding 2 mm incremental tibial rotational levels compiling the entire data set for each specimen. Following the acquisition, the data was analyzed and the results were compared against the study hypothesis to determine the results.

Chapter 7: Experimental Results and Discussion

In order to establish a basis for comparison between the patellar tendon strain trends, the maximum strain undergone by the patellar tendon for each measurement was taken from the recorded data. A summary for all the maximum patellar strain values collected at the control, cut cranial cruciate, and zero, two, four, six, eight, ten, twelve, and fourteen millimeters of rotation of the tibial plateau following a Tibial Plateau Leveling Osteotomy (TPLO) is presented in Table A-1[3]. Five strain measurements were taken for the control, transected cranial cruciate, and all degrees of rotation following the TPLO, to provide a check of the repeatability of the data. The data points were then converted to an average ± standard deviation to provide one data point for each measurement as shown in Table A-2.

A graphical representation of the maximum patellar strain levels is presented in Figure B-19. When graphed, the data shows a strong correlation between the two 18 mm samples and the two 24 mm samples. In order to amplify this apparent relationship, the four samples were split into two charts, Figures B-20 and B-21, that present the two 18 mm and the two 24 mm samples, respectively. To explore the apparent relationship, a Student's t-test was employed to compare all of the recorded data points to each specimen's control. Typically, a Student's t-test uses a standard p-value of 0.05 to check for statistical significance. For this study, there are several t-tests that must be performed to check for significance. If a t-test was run one hundred times, using a p-value of 0.05, then five of the tests would return a false positive against the null hypothesis. Therefore, due to the conformity of the data sets, the p-value was tightened to 0.01 for this study to deter any statistical

[3] All Tables are located in Appendix A.

questions and objections. The resulting p-values for each data set compared to each separate control are presented in Table A-3.

Canine specimens 1 and 2 underwent a TPLO using an 18 mm biradial saw. Therefore, the relationship between the two samples was of interest. After examining Figure B-20, there was an obvious pattern-wise relationship between the two specimens. To further this qualitative relationship, the 24 mm specimens' strain values, presented in Figure B-21, were examined to determine if a similar relationship was identifiable. Although a different pattern from that of the 18 mm pair, there was also a strong visual correlation between the 24 mm data patterns. Statistical analysis was unnecessary due to the remarkable resemblance of the data patterns.

After determining that there were significant differences between the strain levels compared to each of the specimens' controls and that there was a strong correlation between the 18 mm and 24 mm paired specimens, all of the data was related back to each control. The objective of this study was to determine if there was a change in patellar tendon strain following a TPLO. Therefore, to determine if there was a significant change in strain levels after the TPLO, the data was taken and quantified by the maximum values for each measurement as percent differences from the controls as presented in Table A-4. By examining that data, a definitive pattern can be detected. To examine this relationship further, the percent differences were graphed as shown in Figure B-22. It was determined that a TPLO does cause increased strain levels on the patellar tendon.

After the determination was complete that there was a significant change in patellar tendon strain following a TPLO, it was of interest to look at each situation examined with respect to the control to investigate the differences. For the following comparisons, the specimens will be referred to as sample 1

(18 mm dog 1), sample 2 (18 mm dog 2), sample 3 (24 mm dog 3), and sample 4 (24 mm dog 4).

Control – Cut CCL

The cut cranial cruciate ligament did not lead to a statistically significant difference in patellar tendon strain from that of the intact knee in sample 1, 2, or 3. However, sample 4 did show a statistically significant difference from the intact knee. There was approximately a nine (9) percent increase in patellar tendon strain following a cranial cruciate transection. This was interesting because, although the stifle is experiencing increased levels of instability from the ruptured cruciate ligament, in 3 of 4 cases, it is not promoting any change of the patellar tendon strain values throughout the range of applicable flexion. Hasler et.al showed that a transection of the cranial cruciate ligament resulted in reduced muscular loads, knee extensor forces, and range of motion [34]. Therefore, it seems that the CCL will result in a change in knee kinematics, and ultimately, anatomical compensations, but the CCL does not initially directly affect the patellar tendon strain.

Control – 0 mm of tibial plateau rotation following the TPLO

Following the TPLO, there was a statistically significant increase in patellar tendon strain for samples 1, 2, 3, and 4 of approximately 22, 22, 24, and 30 percent from that of the control, respectively. Although there is no change in the geometry of the tibial plateau from that of the cut cranial cruciate, the osteotomy resulted in a 10 to 20 percent increase in patellar tendon strain.

Control – 2 mm of tibial plateau rotation following the TPLO

After the first rotation of 2 mm following the TPLO, there was a statistically significant increase in patellar tendon strain for samples 1, 2, and 3 of approximately 34, 33, and 16 percent, respectively, with respect to the

control. Sample 4 did not show a statistically significant difference, but there was a 15 percent difference between the means. The 18 mm samples experienced approximately a 10 percent increase following the initial 2 mm rotation of the tibial plateau while the two 24 mm samples experienced approximately a 10 percent decrease in patellar tendon strain. This is likely due to the radius of curvature difference between the cuts.

Control – 4 mm of tibial plateau rotation following the TPLO

For 4 mm of tibial plateau rotation following the TPLO, there was a statistically significant increase in patellar tendon strain for samples 1, 2, 3, and 4 of approximately 78, 79, 20, and 20 percent, respectively, with respect to the control. There was a vast increase in patellar tendon strain within the 18 mm samples following 4 mm of tibial plateau rotation, while the 24 mm samples increased more than at 2 mm but less than that of 0 mm.

Control – 6 mm of tibial plateau rotation following the TPLO

Following 6 mm of tibial plateau rotation, there was a statistically significant increase in patellar tendon strain for samples 1, 2, 3, and 4 of approximately 96, 92, 51, and 45 percent, respectively, with respect to the control. At 6 mm of rotation, the strain increase in the patellar tendon had nearly doubled with respect to the control for the 18 mm samples and the 24 mm samples had increased by one and a half times that of the control. This rotation represented the largest amount of patellar tendon strain increase for all angles of rotation for the 18 mm samples.

Control – 8 mm of tibial plateau rotation following the TPLO

Following 8 mm of tibial plateau rotation, there was a statistically significant increase in patellar tendon strain for samples 1, 2, 3, and 4 of approximately 71, 75, 66, and 66 percent, respectively, with respect to the control. Following the peak of patellar tendon strain, the 18 mm samples experienced approximately a 20 percent decrease with the added 2 mm of

rotation. The 24 mm samples continued to increase the patellar tendon strain with respect to the previous degree of rotation.

Control – 10 mm of tibial plateau rotation following the TPLO

After 10 mm of tibial plateau rotation, there was a statistically significant increase in patellar tendon strain for samples 1, 2, 3, and 4 of approximately 45, 41, 61, and 63 percent, respectively, with respect to the control. The 18 mm samples, once again, saw another decrease in patellar tendon strain from the previous level of rotation. The patellar tendon strain in the 24 mm samples remained relatively unchanged from 8 to 10 mm of rotation.

Control – 12 mm of tibial plateau rotation following the TPLO

Following 12 mm of tibial plateau rotation, there was a statistically significant increase in patellar tendon strain for samples 3 and 4 of approximately 81 and 67 percent, respectively, with respect to the control. There was no statistically significant difference in the patellar tendon strain for the 18 mm samples with respect to the control. Although, there was a 15 percent increase between the means for both samples 1 and 2 with respect to the control.

Control – 14 mm of tibial plateau rotation following the TPLO

Following 14 mm of tibial plateau rotation, there was a statistically significant increase in patellar tendon strain for samples 2, 3, and 4 of approximately 29, 20, and 43 percent, respectively, with respect to the control. Sample 1 experienced a statistically significant decrease in patellar tendon strain of approximately 10 percent. At this level of rotation, the relative stability of the knee with respect to the tibia and femur came into question. Such a high angle of tibial plateau rotation resulted in increased macro motion and nonconformity of the data. Therefore, the 14 mm of rotation was not examined in-depth.

Chapter 8: Conclusions

Following a TPLO, the patellar tendon does experience a statistically significant increase in strain. The largest increases for the 18 mm osteotomy were seen at four to eight millimeters of tibial plateau rotation, whereas, the 24 mm osteotomy experienced the greatest increases in patellar strain at the eight to twelve millimeters of tibial plateau rotation. This may provide veterinary surgeons with a better understanding of the kinematic changes seen in the canine stifle following a TPLO. Ordinarily, the angle of rotation is determined prior to surgery by the patient's radiographs. This data will provide more information as to what cut will provide the least patellar tendon strain around those predetermined angles following a TPLO.

The initial hypothesis stated that, "The patellar tendon will experience a change in strain as the tibial plateau geometry is altered following a Tibial Plateau Leveling Osteotomy. It is this change in strain that will be evaluated for the TPLO. By simulation of weight bearing before and after the simulated cranial cruciate rupture and the resulting surgical procedure, strain analysis will provide a pattern of increased or decreased loading as seen by the patellar tendon with respect to the amount of applied rotation to the tibial plateau. This data will provide a basis for understanding the pathology of patellar tendon inflammation, as seen in some patients, after a TPLO." After examining the data, the hypothesis was shown to be correct. Furthermore, the statistically significant differences within each data set from the controlled intact knee provide the study with a strong basis for future work.

It was determined that the weight was not a contributing factor to the patellar tendon strain. During quadriceps flexion, where the patellar tendon strain is at a maximum, the leg is not in a weight bearing position. While the weight of the distal leg below the stifle will affect the results of the patellar tendon strain, it

is not significant. Furthermore, the weight is a parameter that is fixed and will not provide any alternative for improvement of the procedure.

The testing setup needs to be standardized with respect to the attachment to the patella. The rubber section needs to be tight across the patella and tibial crest. Also, when attaching the wire that provides the simulated flexion, a major difficulty that arose during testing was the patellar traction. If the applied force was not in line with the physiological line of force, the patella would lose traction resulting in a twisting effect. This twisting of the sample was unreadable by the strain gage due to the linearity. To remedy this problem, two bone screws should be placed on both the medial and lateral sides of the patella. Now, with the three screws, anterior, medial, and lateral, the patella can be stabilized in traction and no further problems should occur.

While this study provides a good background for the strain seen in the patellar tendon, improvements can be made to continue with the investigation of the TPLO. To improve and expand upon the results, a study plan involving contra lateral legs with different cuts should be employed. This would reduce the physiological variables and provide a measure of the actual values of strain the patellar tendon undergoes following a TPLO. This study provided an investigation of the patterns or percent changes from the controlled intact knee. To perform a study using contra lateral legs would allow a correlation between the 18 mm and 24 mm cuts to be observed. Jones et.al identified that soft tissue material response changed with varying strain rates [35]. Testing should be performed using this knowledge to determine the varying strain levels with respect to changes in angular velocity during flexion.

Following a TPLO, the patellar tendon strain does increase. The increase in strain is directly related to the osteotomy because an intact knee and a knee with a ruptured cranial cruciate resulted in no statistically significant differences in patellar tendon strain. This is further supported by the work of Reiff and Probst

[48]. They determined that there was no difference in tibial plateau angles between intact and cranial cruciate deficient stifles. Although a distinctly different measurement, this leads to a justification that a cranial cruciate deficiency does not result in detrimental changes within the anatomy of the knee.

With respect to preventing any difficulties with the patellar tendon postoperatively, an 18 mm osteotomy should be used for high angles of rotation, 10-14 mm, whereas, a 24 mm osteotomy should be used for 2-6 mm of rotation.

This study should provide veterinary surgeons with a better understanding of the TPLO. Ultimately, this study will provide a basis for future work. Continued research could show that using an optimal cut and rotation combination, which results in a reduction of patellar tendon strain as presented in this study, may lead to a reduction in the amount of patients experiencing adverse effects involving the patellar tendon following a TPLO. With the TPLO being such a widely used procedure, the benefits will be exponential in the reduction of procedures for revisions, consumer costs, and overall health of the patient.

List of References

1) Cordey, J. Gautier, E. Strain Gauges used in Mechanical Testing. *Injury, International Journal of the Care of the Injured*. 30, 1999, Part I pp. 7-13.
2) Cordey, J. Gautier, E. Strain Gauges used in Mechanical Testing. *Injury, International Journal of the Care of the Injured*. 30, 1999, Part II pp. 14-20.
3) Cordey, J. Gautier, E. Strain Gauges used in Mechanical Testing. *Injury, International Journal of the Care of the Injured*. 30, 1999, Part III pp. 21-25.
4) Atkinson, T. Ewers, B. Haut, R. The tensile and stress relaxation responses of human patellar tendon vary with specimen X-Sectional area. *Journal of Biomechanics*. 32, 1999, pp. 907-914.
5) Loren, G. Lieber, R. Tendon biomechanical properties enhance human wrist muscle specialization. *Journal of Biomechanics*. 28, 1995, pp. 791-799.
6) Voigt, M. Bojsen-Moller, F. Simonsen, E. Dyhre-Poulson, P. The influence of tendon Youngs Modulus, dimensions, and instantaneous moment arms on the efficiency of human movement. *Journal of Biomechanics*. 28, 1995, pp. 281-291.
7) Pioletti, D. Rakotomanana, L. The independence of time and strain effects in the stress relaxation of ligaments and tendons. *Journal of Biomechanics*. 33, 2000, pp. 1729-1733.
8) Almekinders, L. Vellema, J. Weinhold, P. Strain patterns in the patellar tendon and the implications for patellar tendinopathy. *Knee*. 10, 2002, pp. 1-5.
9) Sefarth, A. Friedrichs, A. Wank, V. Blickhan, R. Dynamics of the long jump. *Journal of Biomechanics*. 32, 1999, pp. 1259-1267.
10) Konishi, Y. Fukubayashi, T. Takeshita, D. Mechanism of quadriceps femoris muscle weakness in patients with ACL reconstruction. *Scandinavian Journal of Medicine & Science in Sports*. 12, 2002, pp. 371-375.
11) Staubli, H. The quadriceps tendon-patellar bone construct for ACL reconstruction. *Sports Medicine and Arthroscopy*. 5, 1997, pp. 59-67.

12) Pandy, M. Shelburne, K. Dependence of cruciate-ligament loading on muscle forces and external load. *Journal of Biomechanics*. 30, 1997, pp. 1015-1024.

13) Woo, S. Kanamori, A. Zeminski, J. Yagi, M. Papageorgiou, C. Fu, F. The effectiveness of reconstruction of the ACL with the hamstrings and patellar tendon. *Journal of Bone and Joint Surgery*. 84, 2002, pp. 907-914.

14) Silver, F. Ebrahimi, A. Snowhill, P. Viscoelastic properties of self-assembled type I collagen fibers: Molecular basis of elastic and viscous behavior. *Connective Tissue Research*. 42, 2002, pp. 569-580.

15) Tohyama, H. Yasuda, K. The effects of stress enhancement on the extracellular matrix and fibroblasts in the patellar tendon. *Journal of Biomechanics*. 33, 2000, pp. 559-565.

16) Ravalin, R. Mazzocca, A. Grady-Benson, J. Nissen, C. Adams, D. Biomechanical comparison of patellar tendon repair a cadaver model. *The American Journal of Sports Medicine*. 30, 2002, pp. 469-473.

17) Esposito, I. Beard, D. Dodd, C. Shafighian, B. Rehabilitation following patellar tendon or ABC prosthetic ligament reconstruction for chronic ACL deficiency knees. *Knee*. 4, 1997, pp. 81-86.

18) Wren, T. Beaupre, G. Carter, D. A model for load-dependent growth, development, and adaptation of tendons and ligaments. *Journal of Biomechanics*. 31, 1998, pp. 107-114.

19) Pereira, M. Adhikari, A. Patellar tendon injury following ACL reconstruction. *Knee*. 6, 1999, pp. 284-287.

20) Ohno, K. Yasuda, K. Yamamoto, N. Kaneda, K. Hayashi, K. Biomechanical and histological changes in the patellar tendon following *in situ* freezing. *Clinical Biomechanics*. 11, 1996, pp. 207-213.

21) Kyung, H. Ihn, J. Kim, D. Biomechanical properties after pre-twist of canine patellar tendon. International Orthopaedics. 25, 2001, pp. 100-103.

22) Dressler, M. Butler, D. Wenstrup, R. Awad, H. Smith, F. Boivin, G. A potential mechanism for age-related declines in patellar tendon biomechanics. *Journal of Orthopaedic Research*. 20, 2002, pp. 1315-1322.

23) Ahmad, C. Kwak, D. Ateshian, G. Warden, W. Steadman, J. Mow, V. Effects of patellar tendon adhesion to the anterior tibia on knee mechanics. *The American Journal of Sports Medicine*. 26, 1998, pp. 715-724.

24) Berlin, R. Levinsohn, M. Chrisman, H. The wrinkled patellar tendon: an indication in the abnormality of the extensor mechanism of the knee. *Skeletal Radiology*. 20, 1991, pp. 181-185.

25) Provenzano, P. Lakes, R. Keenan,T. Vanderby, R. Nonlinear ligament viscoelasticity. *Annals of Biomedical Engineering*. 29, 2001, pp. 908-914.

26) Zajac, F. Muscle and Tendon: Properties, models, scaling, and application to biomechanics and motor control. *Critical Reviews in Biomedical Engineering*. 17, 1989, pp. 359-407.

27) Fukunaga, T. Kawakami, Y. Kubo, K. Kanehisa, H. Muscle and tendon interaction during human movement. *Exercise and Sports Science Reviews*. 30, 2002, pp. 106-110.

28) Yamamoto, N. Hayashi, K. Mechanical properties of rabbit patellar tendon at high strain rate. *Bio-medical Materials and Engineering*. 8, 1998, pp. 83-90.

29) Capps, G. Hayes, C. Easily missed injuries around the knee. *Radiographics*. 14, 1994, pp. 1190-1210.

30) Woo, S. Debski, R. Withrow, J. Janaushek, M. Biomechanics of knee ligaments. *The American Journal of Sports Medicine*. 27, 1999, pp. 533-543.

31) Chan, K. Qin, L. Hung, L. Tang, C. Li, C. Rolf, C. Alteration of patellofemoral contact during healing of canine patellar tendon after removal of its central third. *Journal of Biomechanics*. 33, 2000, pp. 1441-1451.

32) Kubo, K. Kawakami, Y. Fukunaga, T. Influence of elastic properties of tendon structures on jump performance in humans. *Journal of Applied Physiology*. 87, 1999, pp. 2090-2096.

33) Fukunaga, T. Kawakami, Y. Kubo, K. Kanehisa, H. Measurement of tendon viscoelastic properties *in vivo*. *Scandinavian Journal of Medicine & Science in Sports*. 12, 2002, pp. 3-8.

34) Hasler, E. Herzog, W. Leonard, T. Stano, A. Nguyen, H. In vivo knee joint loading and kinematics before and after ACL transection in an animal model. *Journal of Biomechanics*. 31, 1998, pp. 253-262.

35) Jones, R. Nawana, N. Pearcy, M. Learmonth, D. Bickerstaff, D. Costi, J. Paterson, R. Mechanical properties of the ACL. *Clinical Biomechanics*. 10, 1995, pp. 339-344.

36) Woo, S. Fox, R. Sakane, M. Livesay, G. Rudy, T. Fu, F. Biomechanics of the ACL: Measurements of *in situ* force in the ACL and knee kinematics. *Knee*. 5, 1998, pp. 267-288.

37) Cross, A. Cranial Cruciate Ligament Insufficiency. *Small Animal Advanced Orthopaedic Surgery*. VEM 5432.

38) www.medicalphoto.com. ©2004 all rights reserved.

39) Slocum, B. Slocum, T. Tibial plateau leveling osteotomy for repair of cranial cruciate ligament rupture in the canine. *Veterinary Clinics of North America: Small Animal Practice.* 23, 1993, pp. 777-794.

40) Dejardin, L. Tibial Plateau Leveling Osteotomy. Musculoskeletal System. Pp. 2133-43.

41) Slocum, B. Devine, T. Cranial tibial wedge osteotomy: A technique for eliminating cranial tibial thrust in cranial cruciate ligament repair. *Journal of the American Veterinary Medical Association.* 184, 1984, pp. 564-569.

42) Morris, E. Lipowitz, J. Comparison of tibial plateau angles in dogs with and without cranial cruciate ligament injuries. *Journal of the American Veterinary Medical Association.* 218, 2001, pp. 363-366.

43) Reif, U. et al. Effect of TPLO on stability of the canine cruciate-deficient stifle joint: an *in vitro* study. *Veterinary Surgery.* 31, 2002, pp. 147-154.

44) Slocum, B. Devine, T. Cranial tibial thrust: A primary force in the canine stifle. *Journal of the American Veterinary Medical Association.* 183, 1983, pp. 456-459.

45) Cosgarea, A. et al. Osgood-Schlatter's disease complicating anterior cruciate ligament reconstruction. *Arthroscopy.* 9, 1993, pp. 700-703.

46) Reider, B. et al. Proprioception of the knee before and after ACL reconstruction. *Arthroscopy.* 19, 2003, pp. 2-12.

47) Textbook of Small Animal Orthopaedics, Newton C.D. and Nunamaker D.M. (Eds.) Ithaca: International Veterinary Information Service, 1985;

48) Reif, U. and Probst, C. Comparison of Tibial Plateau Angles in Normal and Cranial Cruciate Deficient Stifles of Labrador Retrievers. *Veterinary Surgery.* Vol. 32, Issue 4, pg. 385, 2003.

Appendix A: Tables

Table A1. MicroStrains of the Patellar Tendon Following a TPLO.

18 mm Dog 1 MicroStrain	Control	Cut CCL	0 mm	2 mm	4 mm	6 mm	8 mm	10 mm	12 mm	14 mm
Mea. 1	600	549	755	806	1081	1201	1030	909	757	534
Mea. 2	584	583	721	806	1064	1167	1063	909	686	534
Mea. 3	635	565	738	824	1081	1149	1047	822	634	551
Mea. 4	617	584	755	824	1098	1219	1030	822	669	568
Mea. 5	601	635	721	806	1081	1219	1030	926	721	551

18 mm Dog 2 MicroStrain	Control	Cut CCL	0 mm	2 mm	4 mm	6 mm	8 mm	10 mm	12 mm	14 mm
Mea. 1	465	480	550	605	830	865	790	651	411	526
Mea. 2	440	440	560	603	820	872	858	637	500	595
Mea. 3	455	435	548	603	800	858	750	635	550	568
Mea. 4	452	450	550	595	785	857	774	670	550	612
Mea. 5	442	475	542	595	785	861	757	568	583	595

24 mm Dog 3 MicroStrain	Control	Cut CCL	0 mm	2 mm	4 mm	6 mm	8 mm	10 mm	12 mm	14 mm
Mea. 1	497	495	600	580	605	740	800	802	905	605
Mea. 2	497	492	626	575	610	743	835	800	905	610
Mea. 3	514	486	615	570	602	754	826	795	900	600
Mea. 4	480	485	625	572	580	752	830	792	893	585
Mea. 5	497	490	624	583	595	756	825	810	897	590

24 mm Dog 4 MicroStrain	Control	Cut CCL	0 mm	2 mm	4 mm	6 mm	8 mm	10 mm	12 mm	14 mm
Mea. 1	620	640	772	687	735	910	1030	960	1030	840
Mea. 2	586	668	800	670	749	841	990	970	1010	858
Mea. 3	605	653	790	590	747	876	990	1008	1030	844
Mea. 4	589	670	738	720	630	850	1010	961	980	858
Mea. 5	603	630	795	750	747	878	960	978	1010	880

*The complete data set for all recorded strain values from the control to the final TPLO rotation for all samples tested.

Table A2. Average MicroStrains Following a TPLO.

MicroStrain±SD	Control	Cut CCL	0 mm	2 mm	4 mm
18 mm Dog 1	607.4±19.3	583.2±32.3	738±17	813.2±9.9	1081±12
18 mm Dog 2	450.8±10.2	456±20.4	550±6.5	600.2±4.8	804±20.4
24 mm Dog 3	497±12	489.6±4.2	618±11	576±5.4	598.4±11.6
24 mm Dog 4	600.6±13.7	652.2±17.4	779±25.2	683.4±60.6	721.6±51.5

MicroStrain±SD	6 mm	8 mm	10 mm	12 mm	14 mm
18 mm Dog 1	1191±31.7	1040±14.8	877.6±51.2	693.4±47.4	547.6±14.2
18 mm Dog 2	862.6±6.1	785.8±43.2	632.2±38.5	518.8±67.2	579.2±33.7
24 mm Dog 3	749±7.1	823.2±13.6	799.8±6.9	900±5.2	598±10.4
24 mm Dog 4	871±27.1	996±26.1	975.4±19.6	1012±20.5	856±15.7

*The average and resulting standard deviations for recorded patellar strain values at each measurement point are presented here.

Table A3. P-values Following Statistical Analysis.

p-value (0.01)	18-dog 1	18-dog 2	24-dog 1	24-dog 2
Cut CCL	0.194	0.629	0.25	0.0008
0 mm Rot.	3.30E-06	3.50E-07	1.70E-07	8.70E-06
2 mm Rot.	7.20E-07	9.80E-08	1.10E-05	0.041
4 mm Rot.	5.60E-10	3.90E-08	8.40E-07	0.0038
6 mm Rot.	3.90E-09	1.60E-11	1.50E-08	1.00E-06
8 mm Rot.	1.70E-09	7.30E-05	1.60E-10	9.10E-08
10 mm Rot.	0.0001	0.00016	5.00E-09	4.00E-09
12 mm Rot.	0.013	0.089	1.20E-08	2.60E-09
14 mm Rot.	0.00084	0.005	5.80E-07	3.40E-09

*The resulting statistical analysis of all strain values compared to their own controls ($p<0.01$).

Table A4. Percent Differences from the Controls.

% Diff from Control	Cut	0	2	4	6
specimen 1	-3.98	21.50	33.88	77.97	96.08
specimen 2	1.33	22.22	33.38	78.67	91.69
specimen 3	-1.48	24.36	15.91	20.41	50.72
specimen 4	8.70	29.83	13.90	20.27	45.17

% Diff from Control	Cut	8	10	12	14
specimen 1	-3.98	71.22	44.49	14.16	-9.84
specimen 2	1.33	74.62	40.49	15.29	28.71
specimen 3	-1.48	65.65	60.94	81.10	20.33
specimen 4	8.70	66.00	62.57	68.67	42.67

*The resulting percent differences of each strain measurement with respect to each control.

Appendix B: Figures

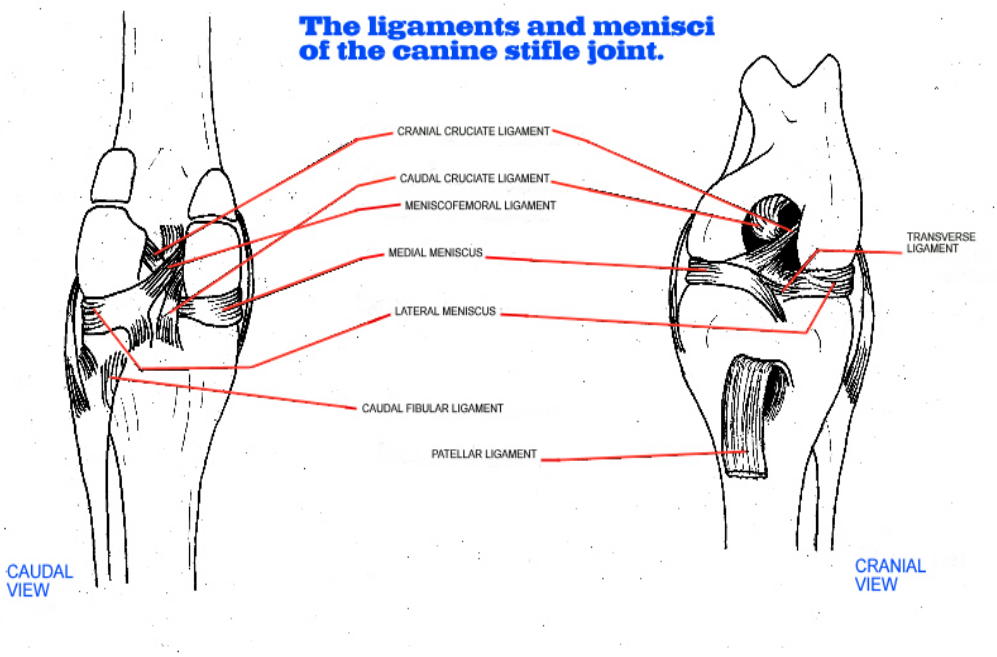

Figure B1. Anatomy of the Canine Stifle.

Figure B2. Radiograph of a Normal Intact Knee [38].

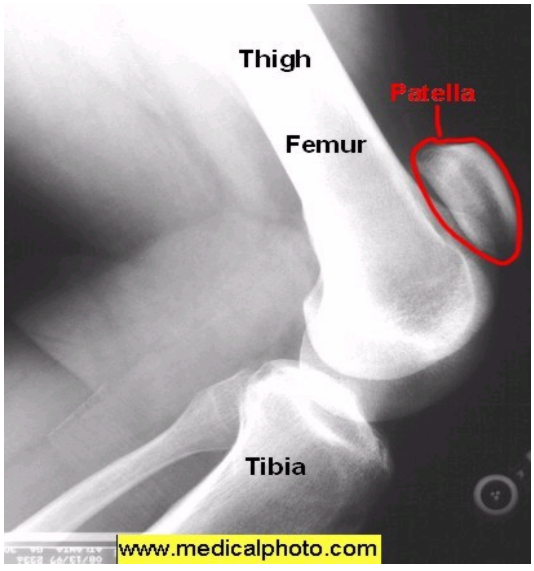

Figure B3. Radiograph of a Knee Following a PT Rupture [38].

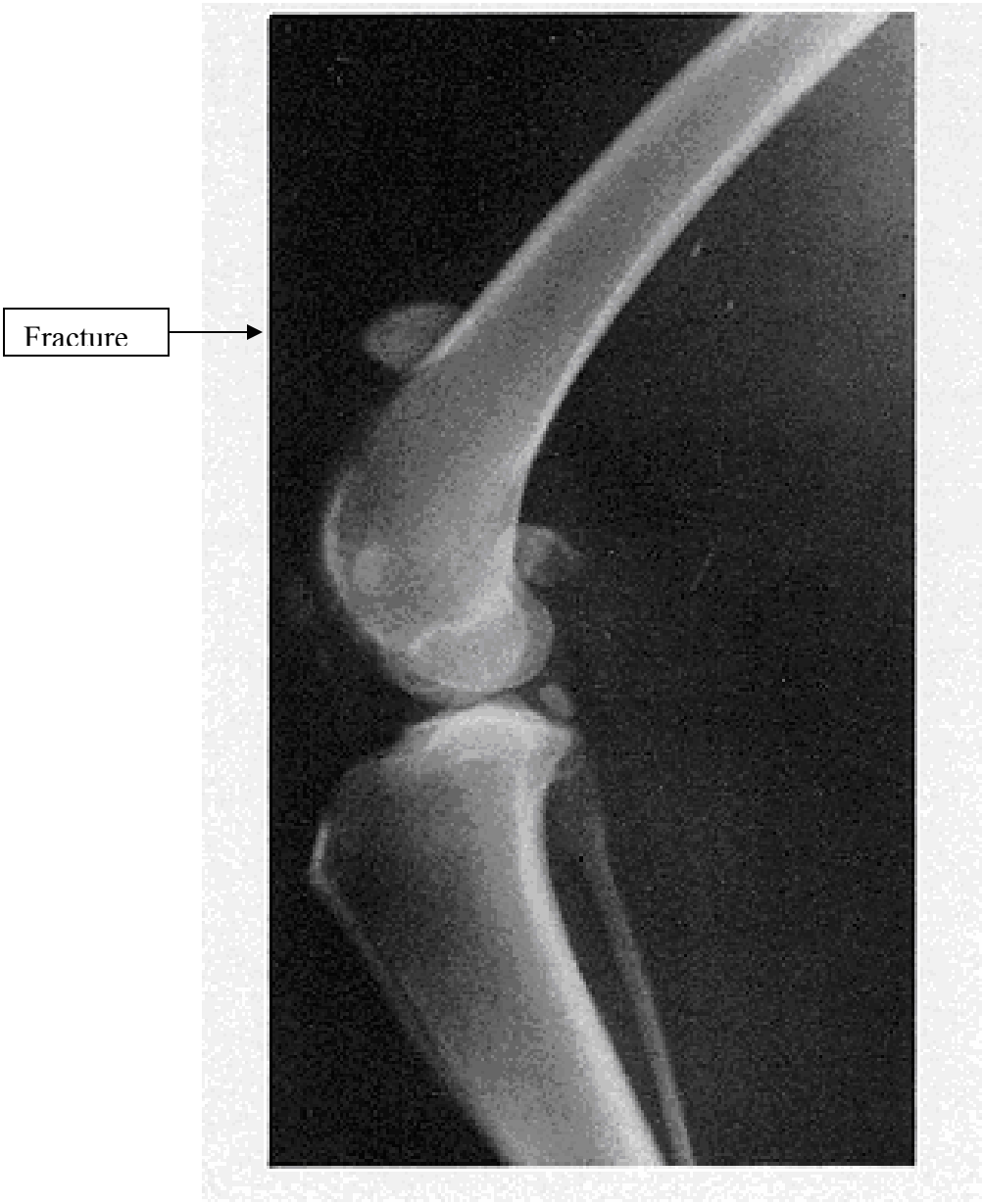

Figure B4. Radiograph of a Comminuted Fracture of a Canine Patella.

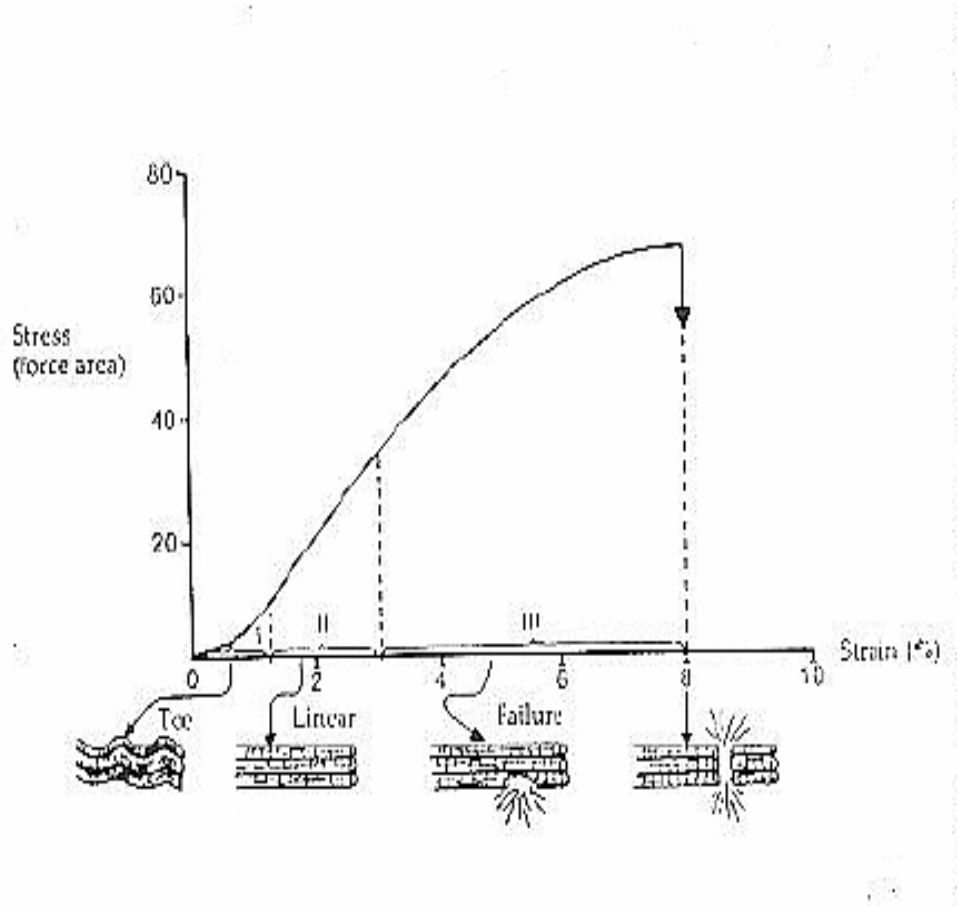

Figure B5. Stress-Strain Curve of the Human Patellar Tendon (26).

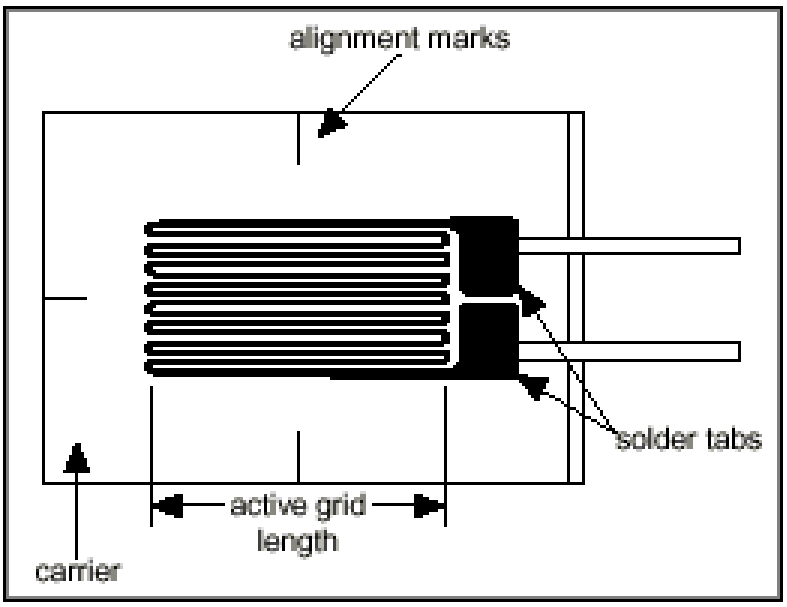

Figure B6. A Diagram of a Strain Gage.

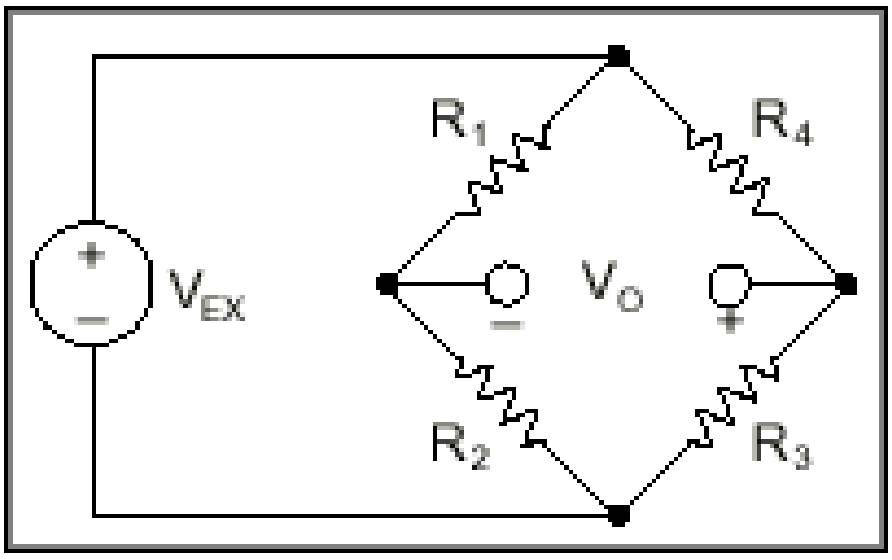

Figure B7. A Classical Wheatstone Bridge.

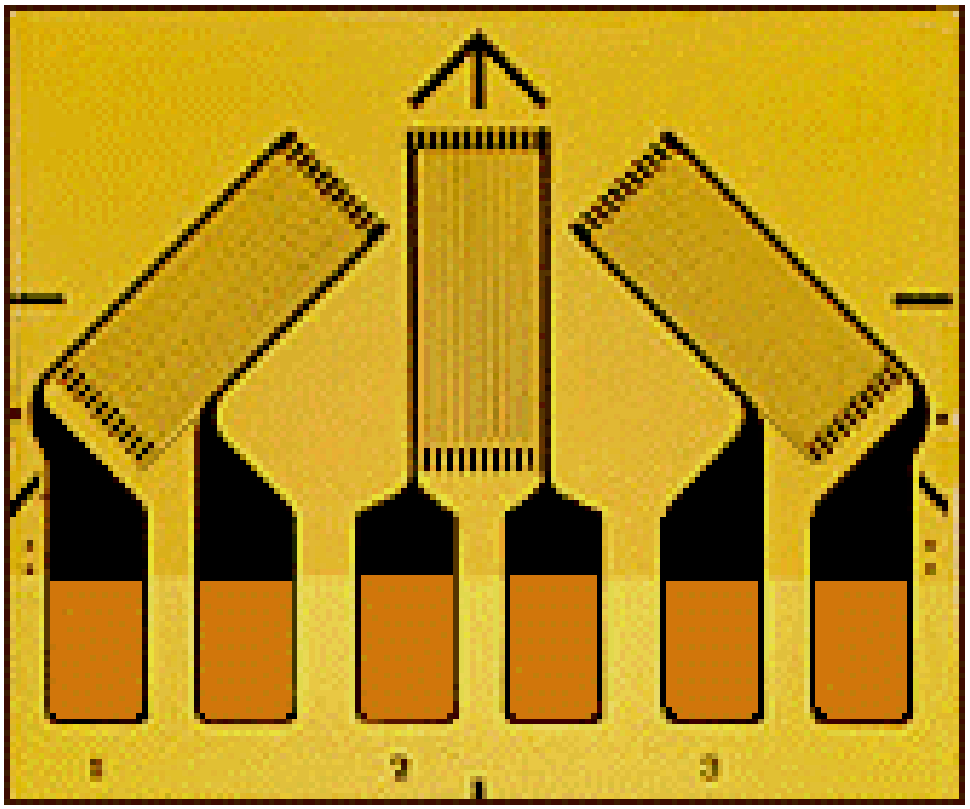

Figure B8. A 45-degree Strain Gage Rosette.

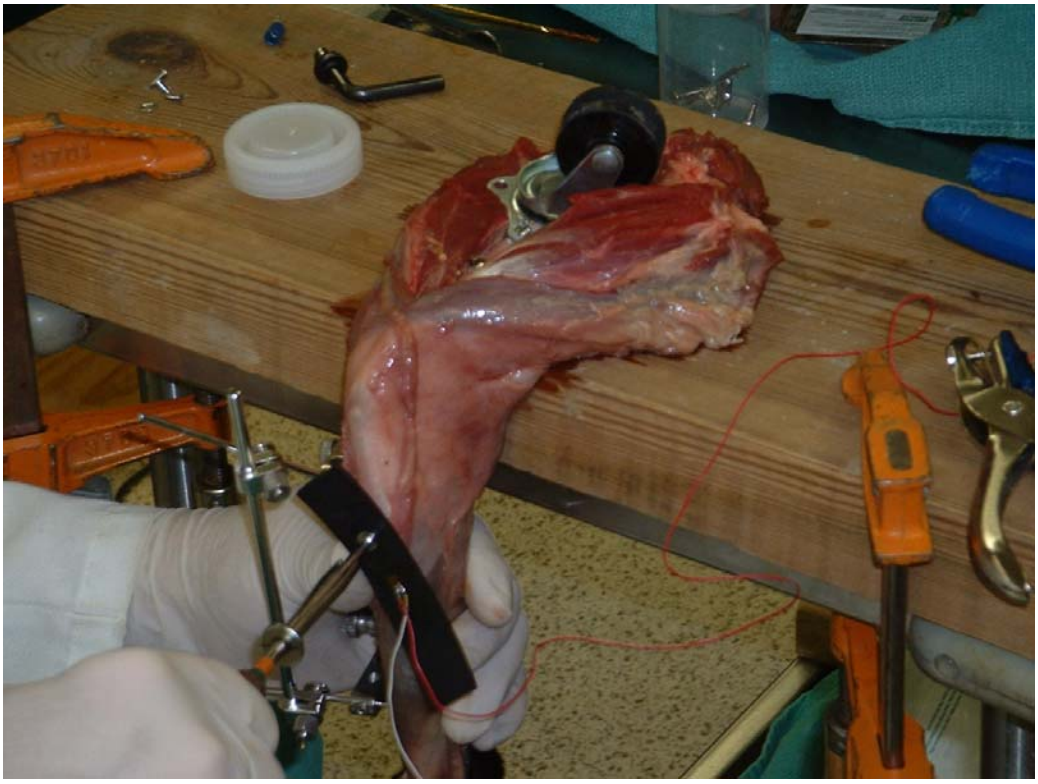

Figure B9. Mounting for the Cadaver Specimen.

*An image showing the mounting setup for stabilizing the cadaver prior to testing.

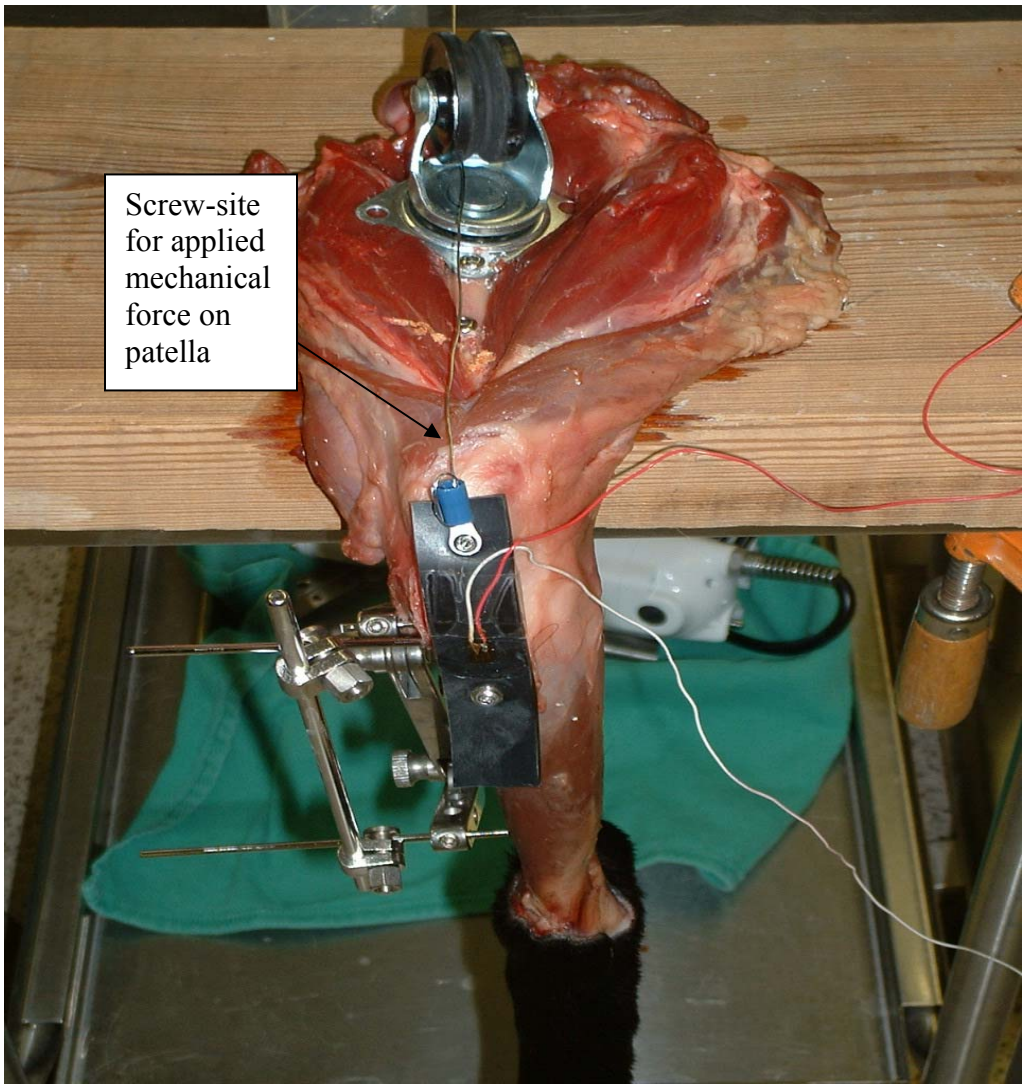

Figure B10. Bone Screw Through the Patella for Wire Attachment.

*An image showing the bone screw thru the patella for attachment of the wire applying the mechanical stimulus to the system.

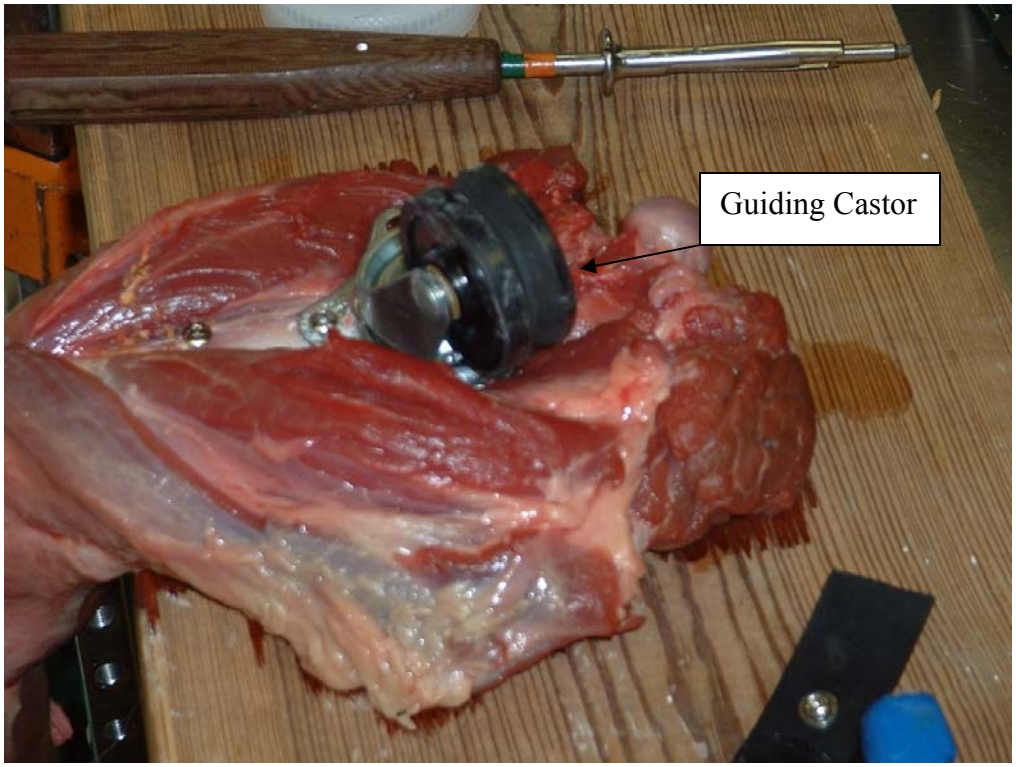

Figure B11. Castor for Aiding Patellar Traction.

*An image of the castor attached to the mid-shaft of the anterior femur for wire guidance during application of the mechanical force.

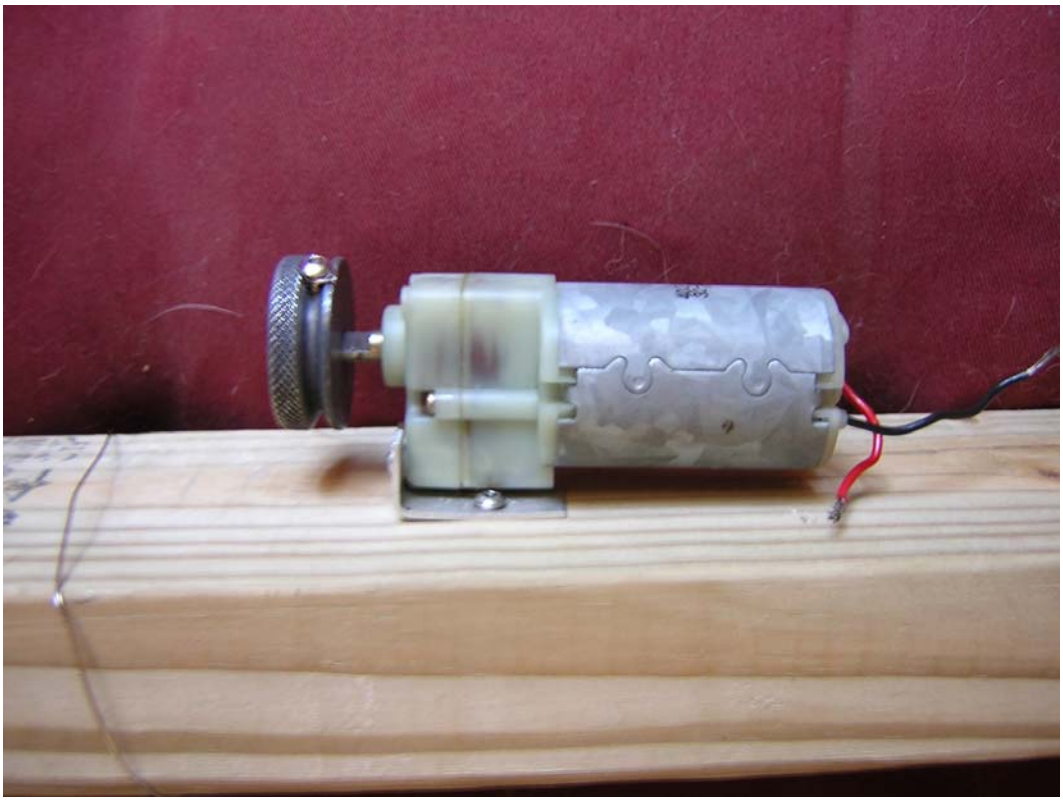

Figure B12. Servomotor.

*An image of the servomotor used to simulate the muscle contraction force required for stifle flexion.

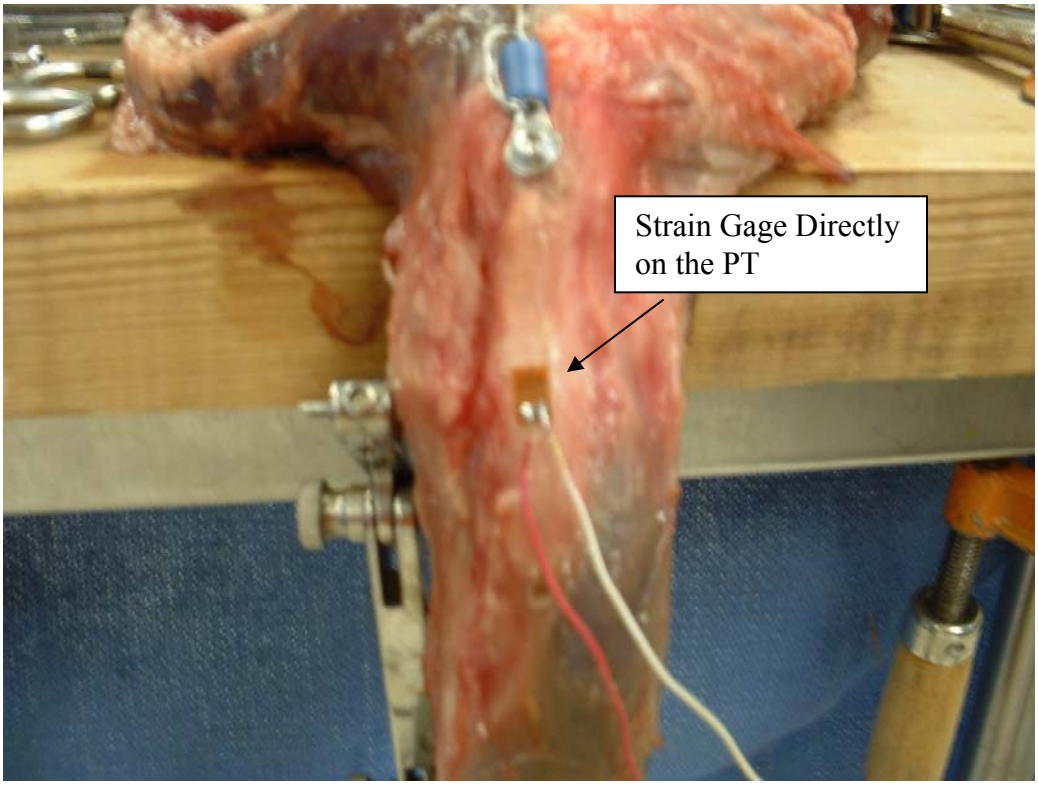

Figure B13. Strain Gage on the Patellar Tendon.

*An image showing the strain gage applied directly to the patellar tendon.

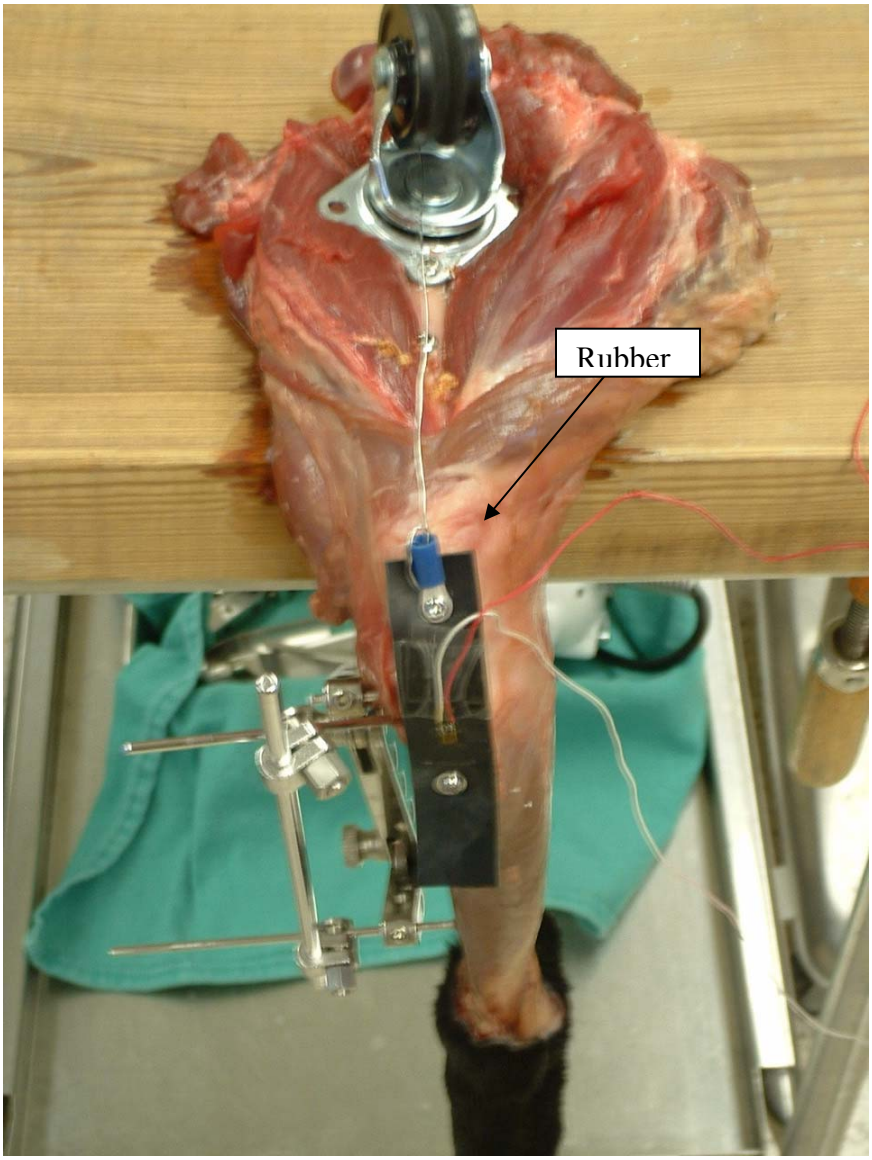

Figure B14. Rubber Section for Simulating the Patellar Tendon.

*An image showing the rubber attached at the patella and tibial crest. The rubber was used to simulate a controlled patellar tendon strain.

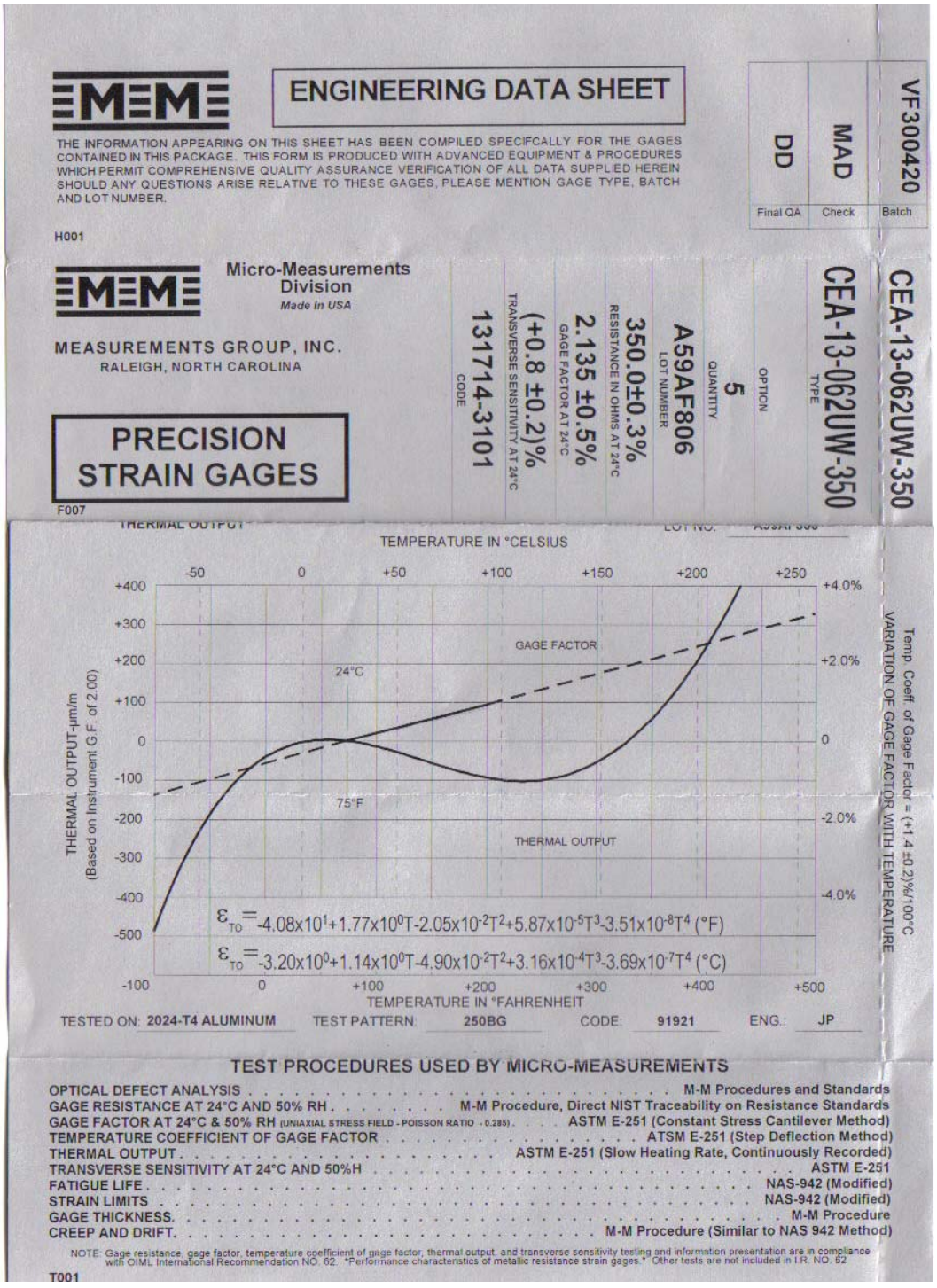

Figure B15. Strain Gage Engineering Data Sheet.

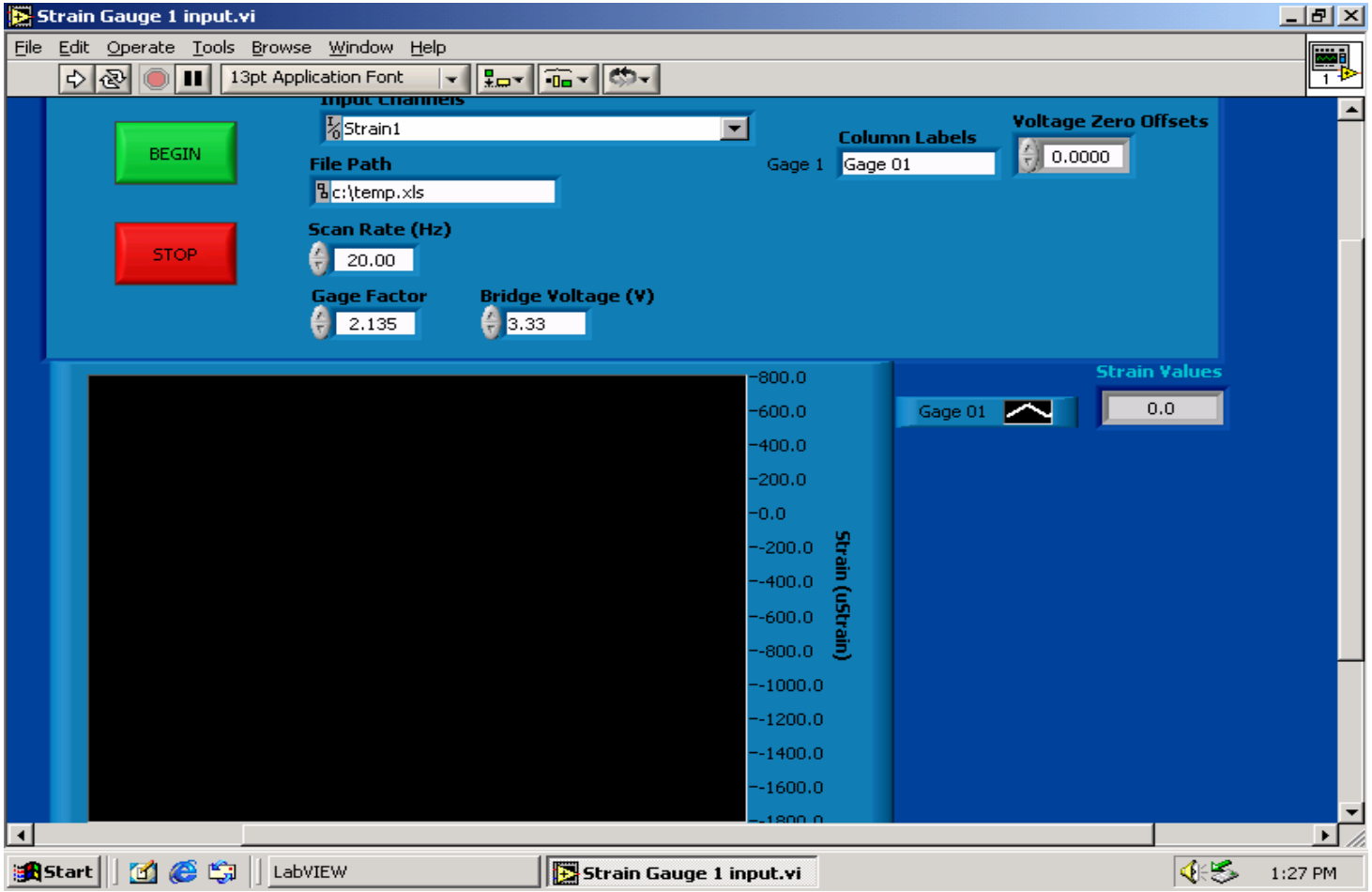

Figure B16. LabVIEW® Front Panel.

*This image represents the front panel controls for the LabVIEW® data acquisition program.

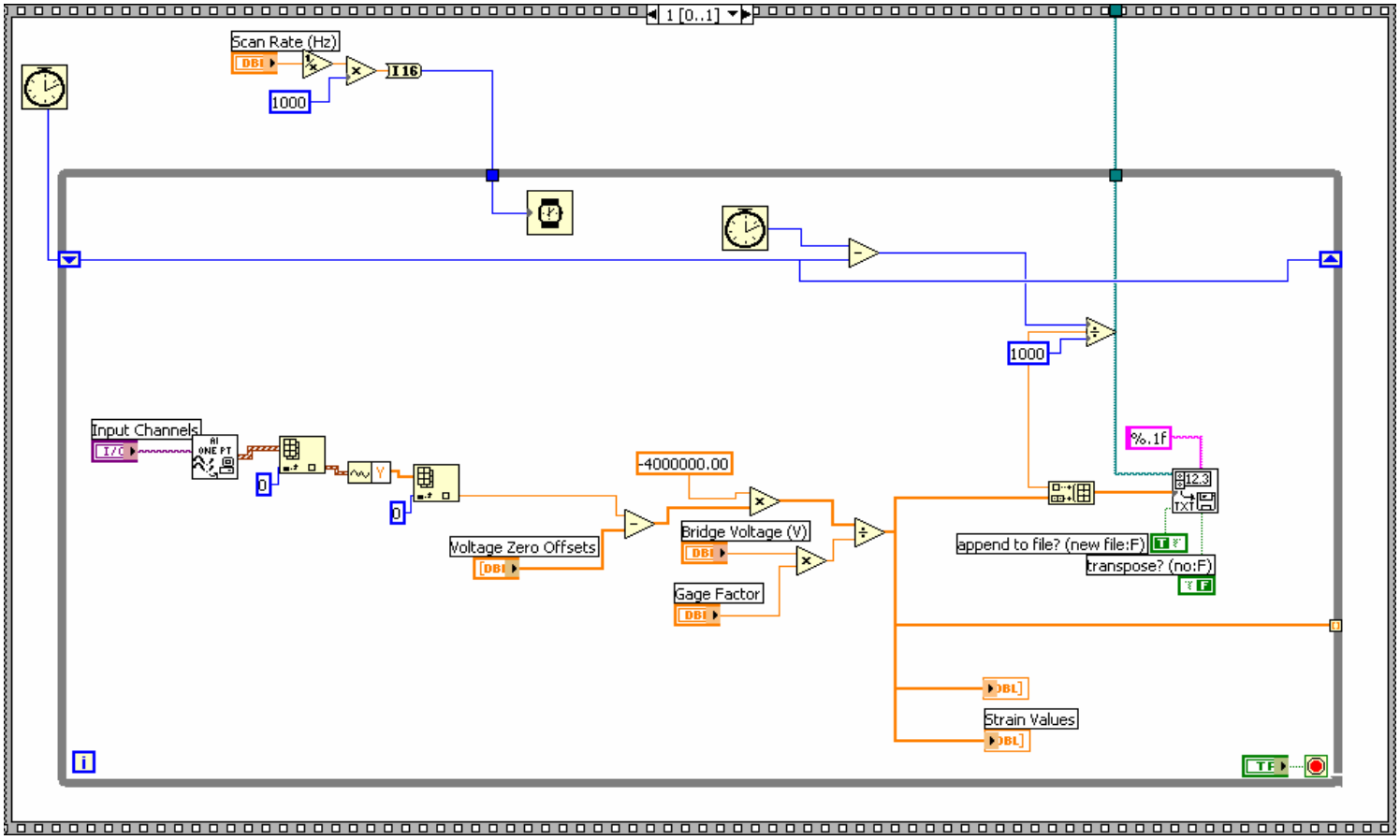

Figure B17. LabVIEW® Programming Panel.

*This image displays the programming panel for the LabVIEW® program.

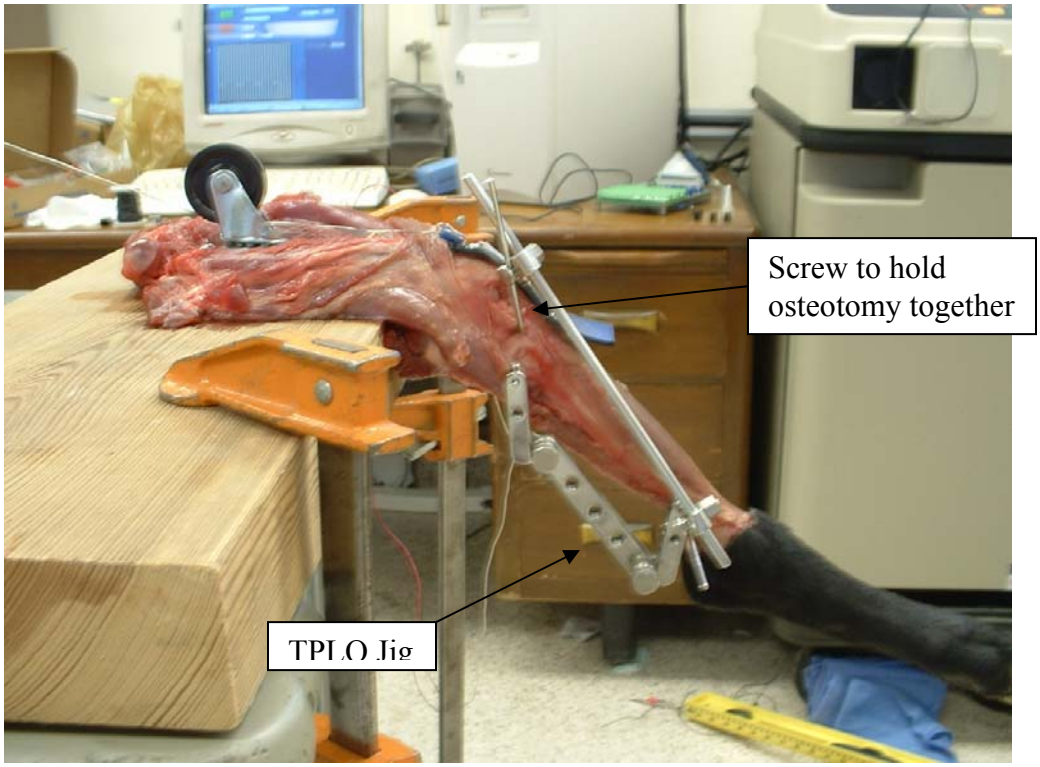

Figure B18. Bone Plate Substitute for TPLO.

*An image showing the jig and screws that hold the osteotomy together without having to attach the bone plate.

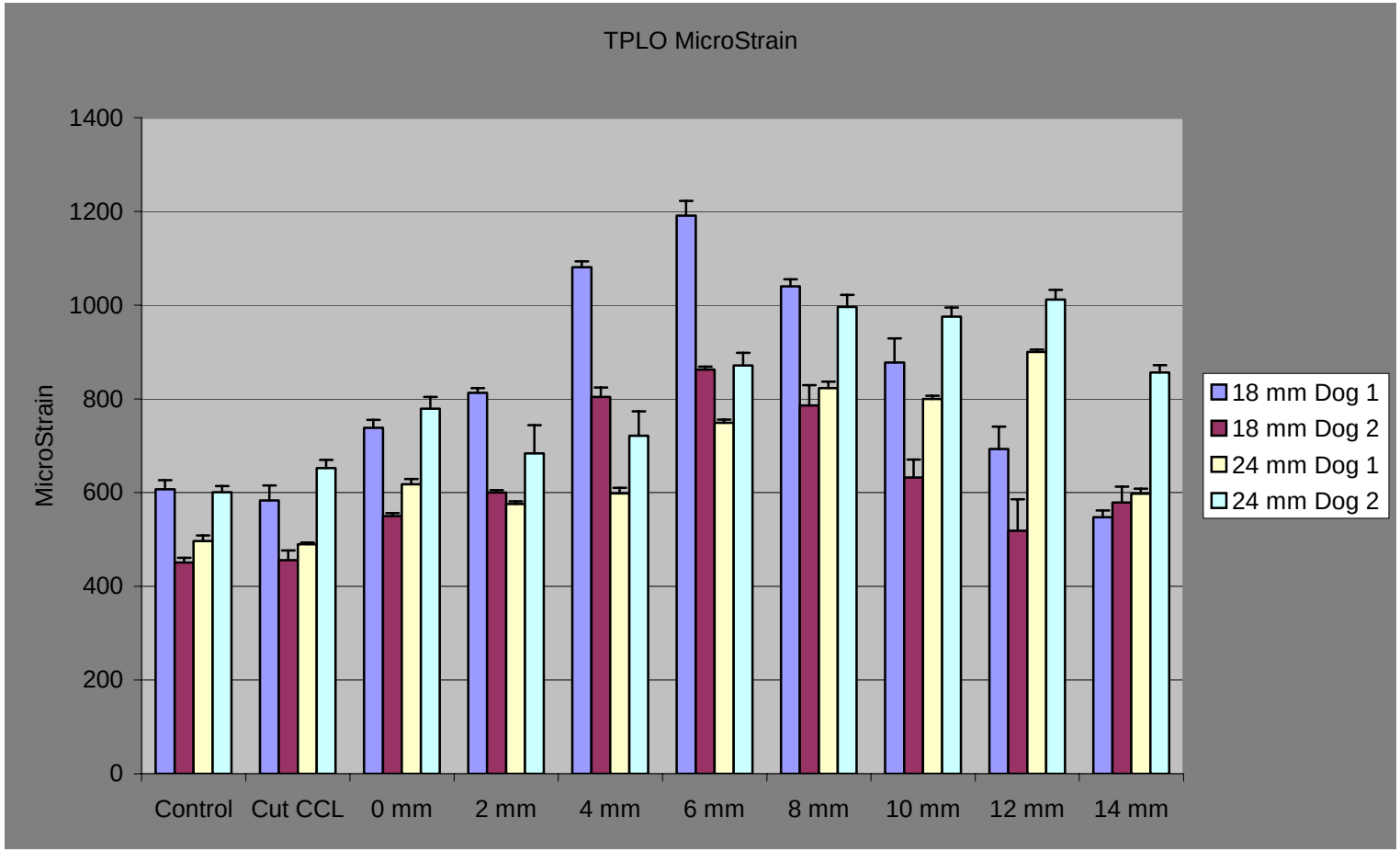

Figure B19. TPLO MicroStrains.

*All of the average maximum patellar strain values recorded for all four samples.

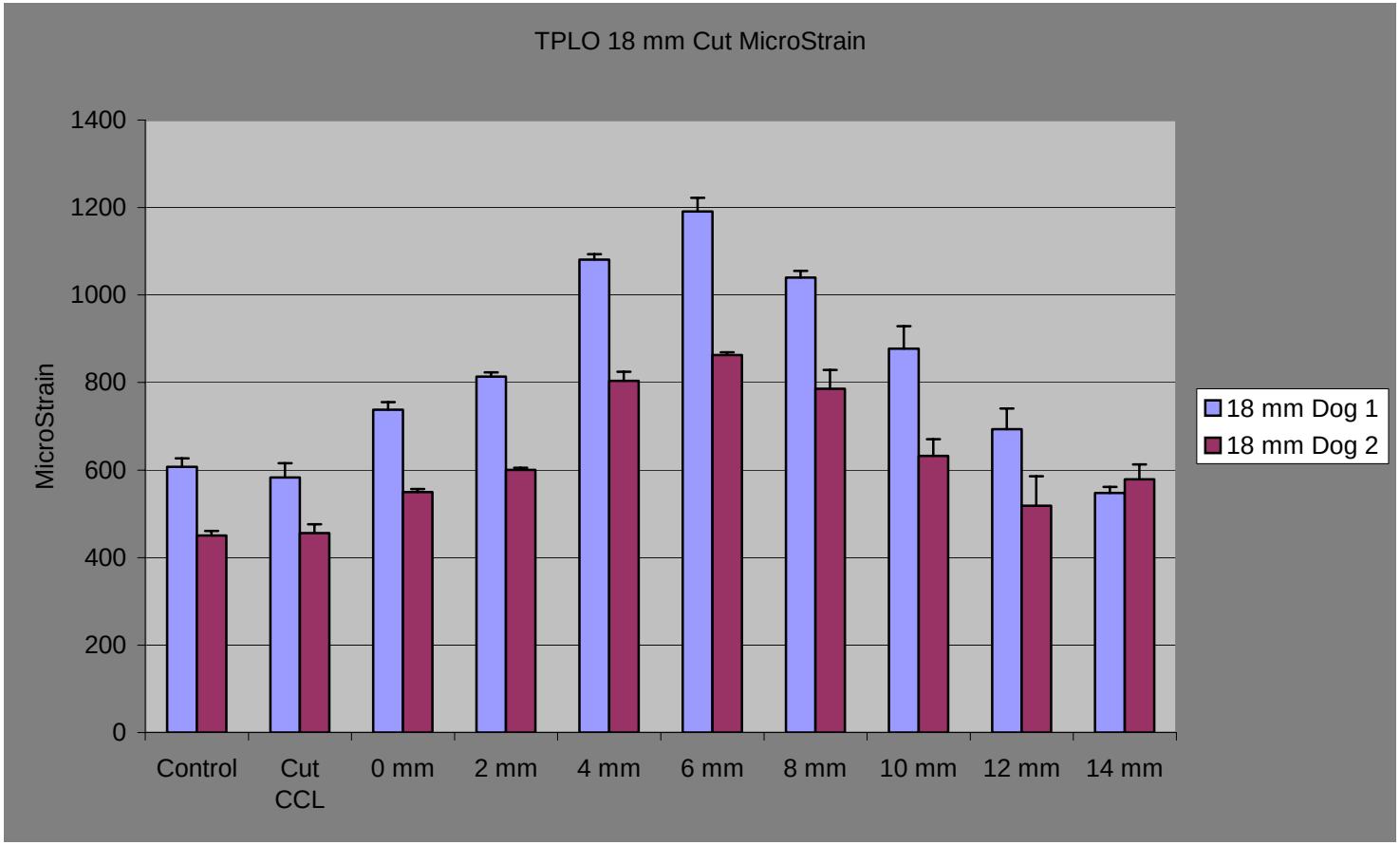

Figure B20. TPLO 18 mm Cut MicroStrains.

*The 18 mm samples showing maximum strain values and their apparent relationship.

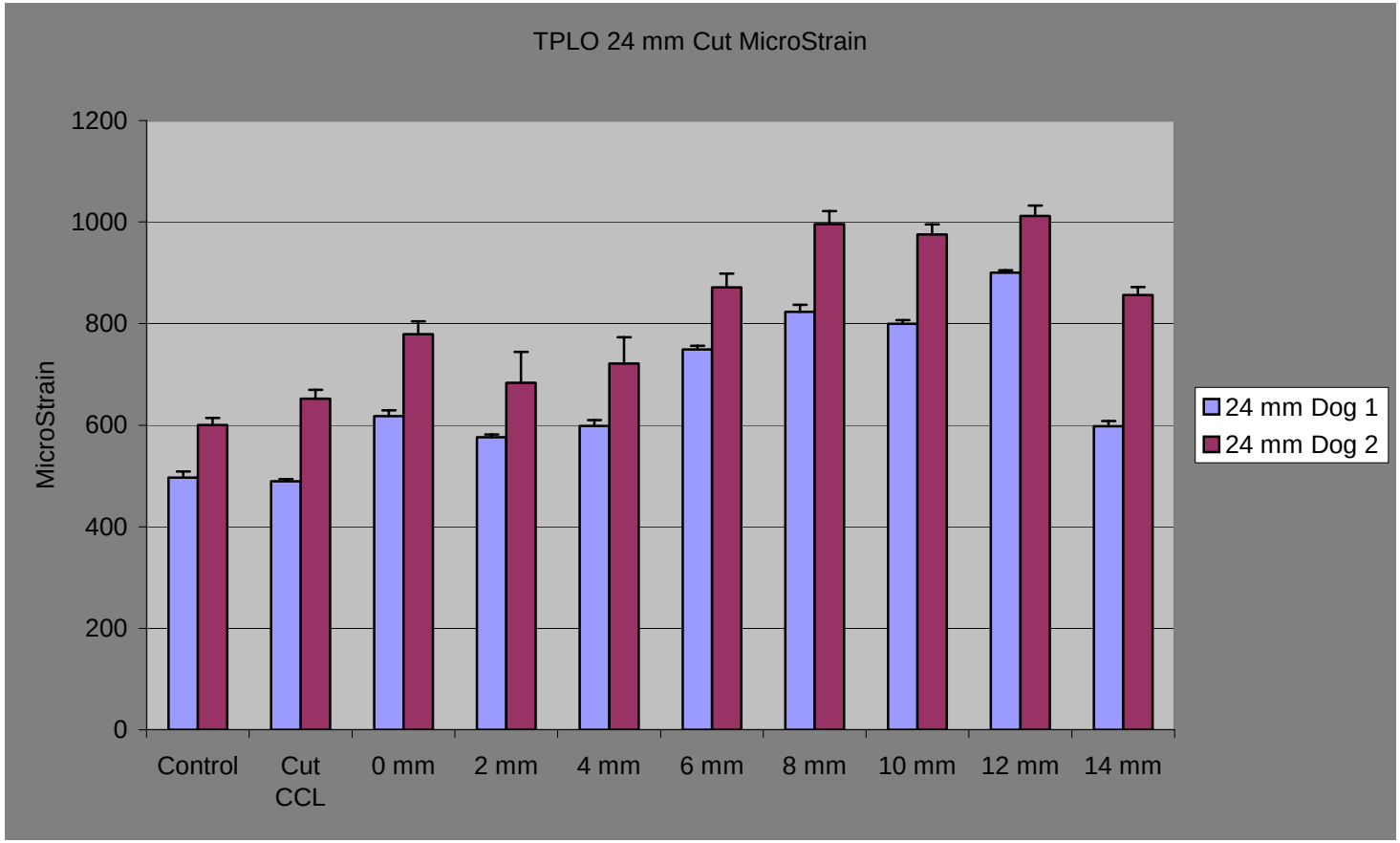

Figure B21. TPLO 24 mm Cut MicroStrains.

*The 24 mm samples showing maximum strain values and their apparent relationship.

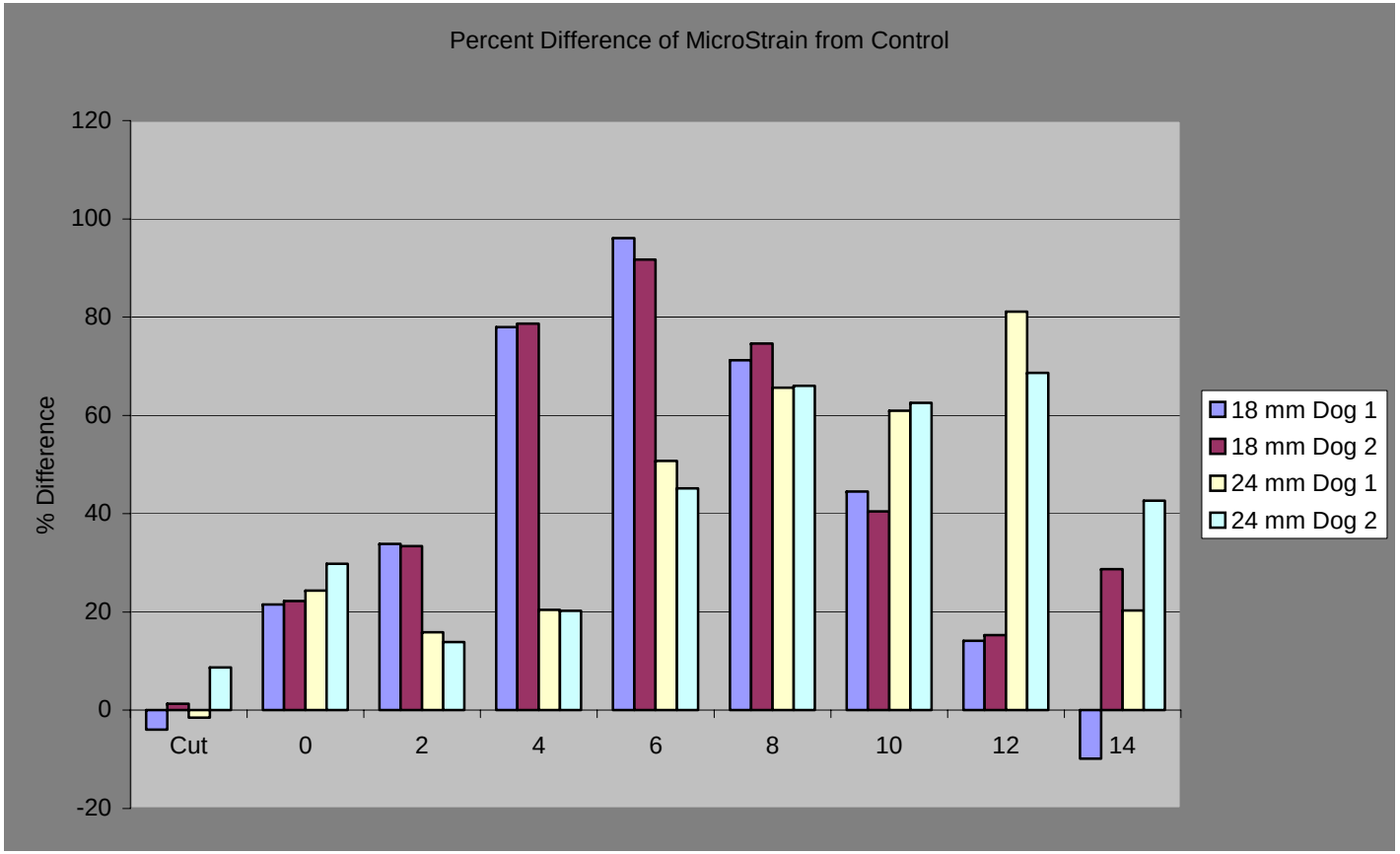

Figure B22. Percent Differences of MicroStrains from Control.

*A diagram showing the percent differences of patellar tendon strain with regards to their respective controls.

Appendix C: Study Plan

Problem Statement

Straight patellar ligament desmitis occurs frequently following a TPLO procedure. Cause is unknown.

Fracture of the tibial tuberosity also occurs but with less frequency. Pathogenesis is unknown.

Hypothesis

Rotation of the tibial plateau increases the tensile strain on the straight patellar ligament.

Rotation of the tibial plateau causes bending of the tibial tuberosity.

Review of the Literature

Standard of surgical therapy.

Theoretical Basis

Establish relationship between tensile strain and ligament injury.

Description of the mechanical basis of the TPLO and its influence on the tensile strain of the straight patellar ligament.

As the tibial plateau is rotated, the centroid of the stifle (located near the center of the femoral condyles) is shifted toward the patella and the patellar ligament. The femur pushes the patella forward increasing tension on the patellar ligament. This increased tension causes limited structural micro-failure of the ligament, which is observed as a reactive inflammation (desmitis) of the ligament.

Description of the mechanical basis of the TPLO and its influence on the bending stresses of the tibial tuberosity.

As a result of the circular osteotomy, the tibial tuberosity is separated from the tibial plateau. As the stifle flexes, the direction of the tensile force on the tibial tuberosity is shifted causing the tuberosity to bend over the cranial edge of the rotated tibial plateau.

Materials and Methods

Procedure

TPLO (18-mm and 24-mm blades) is performed in the standard method. Strain gauges attached to a rectangular uniform piece of rubber simulating the straight patellar ligament by attachment at the patella and the tibial crest. Tibial plateau is rotated at 2-mm intervals and strain is recorded at each level under the following conditions.

Spring simulation of quadriceps function with:

Stifle in weight bearing angle. Stifle in multiple flexion angles. The two steps above are repeated with the cranial cruciate ligament transected. TPLO (24-mm blade) is done on contra lateral stifle and the study is repeated.

Cadaver Study

Intact cruciate ligament in a weight bearing stifle flexion angle with maximal flexion of the hock and a full range of motion. Two groups: 18 and 24 mm groups of 2 stifles each. Compare maximum strain vs. plateau displacement within each group. Compare groups 18 mm vs. 24 mm. Intact cranial cruciate ligament during range of motion of the stifle.

Two groups: 18 and 24 mm groups of 2 stifles each

Compare strain vs. plateau displacement within each group.

Compare groups 18 mm vs. 24 mm

Transected cranial cruciate ligament in a weight bearing stifle flexion angle with maximal flexion of the hock and a leg weight bearing force.

Two groups: 18 and 24 mm groups of 2 stifles each. Compare strain vs. plateau displacement within each group. Compare groups 18 mm vs. 24 mm. Transected cranial cruciate ligament during range of motion of the stifle.

Two groups: 18 and 24 mm groups of 2 stifles each. Compare strain vs. plateau displacement within each group. Compare groups 18 mm vs. 24 mm

Detailed Method

Four cadaver dogs, ranging in weight from 50 to 80 #s, with normal stifle joints. A servo motor and high tension steel wire will apply the load to simulate the physiological range of motion.

A longitudinal incision is made from the proximal aspect of the patella to 15 cm proximally on the cranial surface of the femur. The incision is carried down through the muscle to the bone. Two small "eye" screws are placed into the patella. Two more "eye" screw is placed into the shaft of the femur to anchor a castor pulley for the wire to run through to simulate the normal loading angle of the patellar tendon. The wire is hooked to the "eye" screws and the load is applied.

Threaded pins are applied to the greater trochanter, lateral femoral epicondyle, and distal tibia proximal to the lateral malleolus. The trochanteric and tibial pins are connected with two rods and bolted clamps.

An area on the cranial surface of the straight patellar ligament is exposed for the application of a strain gauge. The skin is closed over the gauge.

An area on the cranial surface of the proximal tibia and distal to the attachment of the quadriceps is exposed by denuding and drying the bone for the application of a strain gauge with tissue adhesive.

Tibial plateau leveling and data acquisition

An area over the medial aspect of the proximal tibia is exposed by lifting and retracting the pes anserinus.

Prior to osteotomy, strain values are obtained for the intact stifle, which will serve as the control values.

The osteotomy jig is applied and an osteotomy is made with the 18-mm biradial blade. The distal osteotomy line is marked with an osteotome at 2-mm intervals ranging over a length of 0 - 14 mm. The proximal ostoetomy line is marked once at the 0 point. A rotation lever pin is applied to the proximal

segment and a 0.062" diameter fixation pin, applied from medial to lateral, is also applied.

Strain values are obtained using the same sample of rubber as the control for rotation at the 0 point followed by 2-mm increment up to and including the 14-mm displacement point.

The procedure is repeated on the contra lateral side with a 24-mm biradial blade.

Results

Spread sheet design.

Description of statistical analysis.

Discussion

Mechanics of stifle with normal cranial cruciate ligament.

Mechanics of stifle with cranial cruciate ligament deficiency.

Mechanics of TPLO and its influence on the straight patellar ligament and tibial tuberosity.

Conclusion

Summary Statement.

Recommendations for Future Study

Implications of this study's findings.

Future recommendations.

Appendix D: Alternative Testing Not Used in Study

The following diagrams and chart show the testing setup for the calibration and validation steps for assigning a known usable value to the outputs recorded by the strain gages. It was determined that the values were not an issue that was required to answer the questions within the scope of this study. Therefore, the method was stopped and the testing proceeded in another manner. It may be possible that this information is useful in continuing studies.

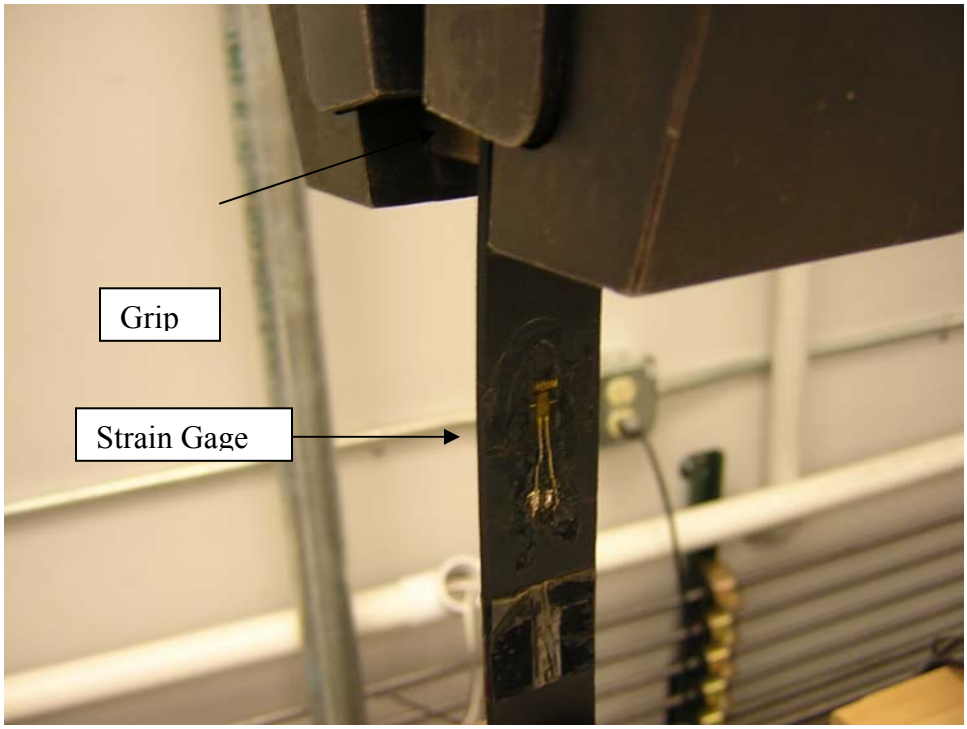

Figure D1. Wedge Grip and Strain Gage Location.

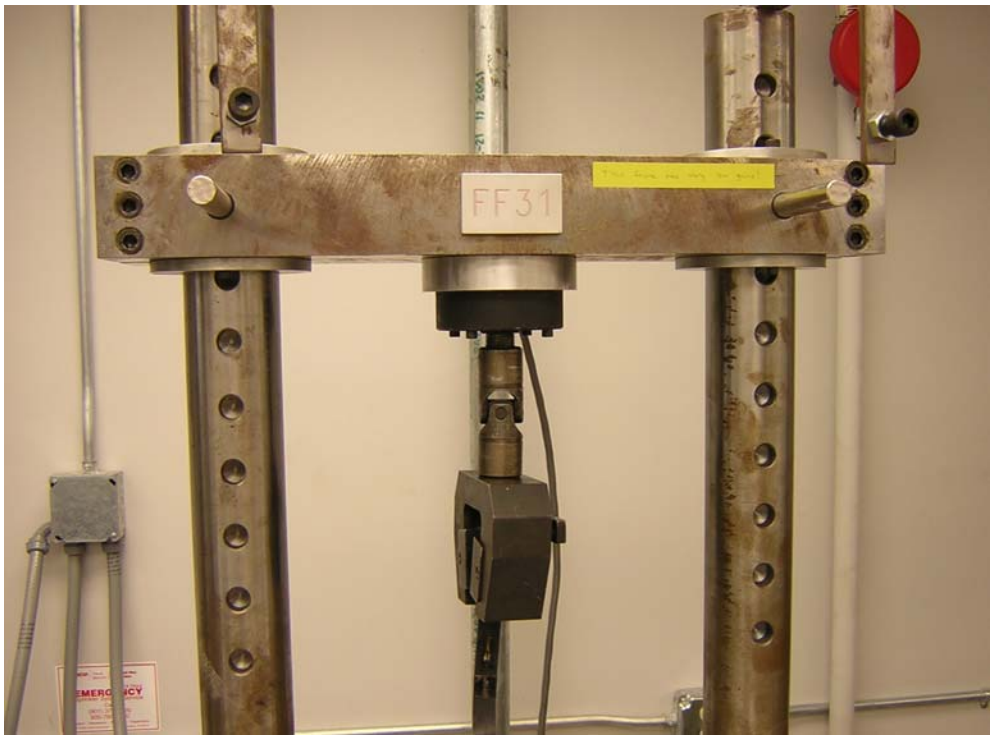

Figure D2. 858 MTS Setup.

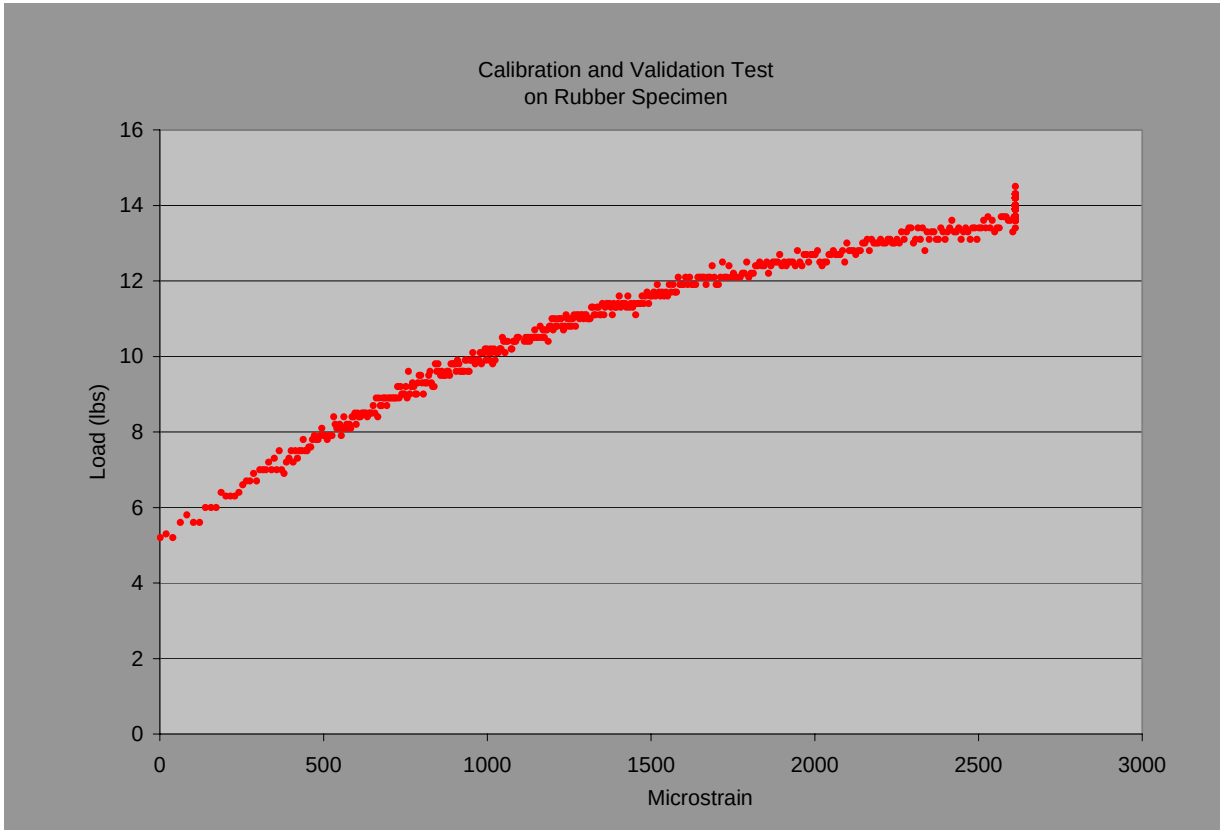

Figure D-3. Load versus Deformation Validation Curve.
* This became a non-issue for this study.

Vita

Joshua Paul Stapleton was born and raised in Kingsport, TN beginning April 24, 1979. He attended grade and junior high school at Indian Springs and Ross and Robinson, respectively. He graduated from Dobyns-Bennett High School in 1997. Thereafter, he went to the University of Tennessee at Knoxville and earned a Bachelor of Science degree in Biomedical Engineering with a minor in Business Administration in 2002. While working with the Veterinary Hospital during his undergraduate work, an opportunity for research became available. This research led to him staying at the University of Tennessee and earning a Masters of Science degree in Engineering Science in 2004.

Josh is currently working in knee manufacturing for Smith & Nephew, Inc. Orthopaedics Division in Memphis, TN. He is also pursuing his MBA in at the University of Memphis. His projected graduation is in 2006.